Journal of
Medicinal Chemistry

Subscriber access provided by BUFFALO STATE

Article

Discovery of 4-Aminoquinoline-3-carboxamide Derivatives as Potent Reversible Bruton's Tyrosine Kinase Inhibitors for the Treatment of Rheumatoid Arthritis

Xia Yao, Xiuyun Sun, Shuyu Jin, Ling Yang, Hongjiang Xu, and Yu Rao

J. Med. Chem., **Just Accepted Manuscript** • DOI: 10.1021/acs.jmedchem.9b00329 • Publication Date (Web): 01 Jul 2019

Downloaded from http://pubs.acs.org on July 1, 2019

Just Accepted

"Just Accepted" manuscripts have been peer-reviewed and accepted for publication. They are posted online prior to technical editing, formatting for publication and author proofing. The American Chemical Society provides "Just Accepted" as a service to the research community to expedite the dissemination of scientific material as soon as possible after acceptance. "Just Accepted" manuscripts appear in full in PDF format accompanied by an HTML abstract. "Just Accepted" manuscripts have been fully peer reviewed, but should not be considered the official version of record. They are citable by the Digital Object Identifier (DOI®). "Just Accepted" is an optional service offered to authors. Therefore, the "Just Accepted" Web site may not include all articles that will be published in the journal. After a manuscript is technically edited and formatted, it will be removed from the "Just Accepted" Web site and published as an ASAP article. Note that technical editing may introduce minor changes to the manuscript text and/or graphics which could affect content, and all legal disclaimers and ethical guidelines that apply to the journal pertain. ACS cannot be held responsible for errors or consequences arising from the use of information contained in these "Just Accepted" manuscripts.

is published by the American Chemical Society. 1155 Sixteenth Street N.W., Washington, DC 20036

Published by American Chemical Society. Copyright © American Chemical Society. However, no copyright claim is made to original U.S. Government works, or works produced by employees of any Commonwealth realm Crown government in the course of their duties.

Discovery of 4-Aminoquinoline-3-carboxamide Derivatives as Potent Reversible Bruton's Tyrosine Kinase Inhibitors for the Treatment of Rheumatoid Arthritis

Xia Yao,[1, ‡] Xiuyun Sun,[1,2, ‡] Shuyu Jin,[3] Ling Yang,[4] Hongjiang Xu,[4] and Yu Rao [1, *]

[1]Ministry of Education (MOE) Key Laboratory of Protein Sciences, School of Pharmaceutical Sciences, MOE Key Laboratory of Bioorganic Phosphorus Chemistry & Chemical Biology, Tsinghua University, Beijing 100084, P.R. China.

[2]Tsinghua-Peking Center for Life Sciences, Beijing 100084, P.R. China.

[3]Key Laboratory of Structure-Based Drugs Design & Discovery of Ministry of Education, Shenyang Pharmaceutical University, Shenyang 110016, P.R. China.

* Corresponding author. e-mail: yrao@tsinghua.edu.cn

‡ These authors contributed equally to this manuscript.

[4]R&D Institute, Chia Tai Tianqing Pharmaceutical Group Co.,LTD, Nanjing 210023, P.R. China.

KEYWORDS. Structure hopping, Reversible BTK inhibitors, 4-Aminoquinoline-3-carboxamide derivatives, Rheumatoid arthritis

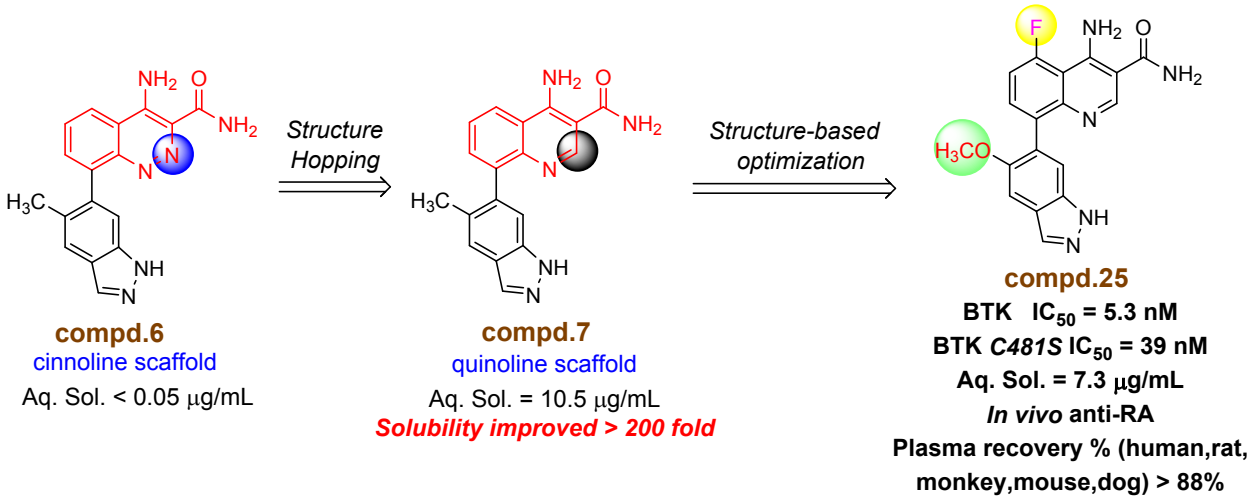

ABSTRACT. A structure-hopping strategy was applied to discover a series of novel 4-aminoquinoline-3-carboxamide derivatives as potent, reversible BTK inhibitors. Compared to the previously described cinnoline scaffold compounds, the 4-aminoquinoline analogs showed significantly improved drug-like properties, especially in their aqueous solubility. The most potent compound, **25**, displayed a stronger inhibitory

effect on both BTK^{WT} (IC_{50} = 5.3 nM) and BTK^{C481S} (IC_{50} = 39 nM). In a rodent collagen-induced arthritis model, compound **25** efficiently reduced paw swelling without a loss in body weight. On the basis of potency, drug-like properties, stability and noncovalent mode of inhibition, our representative inhibitors could have a promising profile to be treatments for a wide range of autoimmune diseases.

INTRODUCTION.

Rheumatoid arthritis (RA) is a multifactorial autoimmune disease that can cause serious cartilage destruction and bone erosion.[1] Therapeutic medications for RA include nonsteroidal anti-inflammatory drugs (NSAIDs), disease-modifying antirheumatic drugs (DMARDs), TNF alpha inhibitors, IL-6 inhibitors, T-cell activation inhibitors, B-cell depleters, immunosuppressants, etc.[2] Tofacitinib, a JAK1/3 inhibitor, was approved by the FDA in 2012 and served as the first kinase inhibitor for the treatment of autoimmune diseases. It has been reported that tofacitinib has similar efficacy to adalimumab in RA patients who show a poor response to methotrexate (MTX) administration.[3] The

success of tofacitinib motivated us to search for other kinase targets that are implicated in RA.[4] Recently, several findings suggested that inhibiting the activity of Bruton's tyrosine kinase (BTK) could provide a promising treatment profile for autoimmune diseases such as RA and systemic lupus erythematosus (SLE).[5,6] BTK belongs to the Tec non-receptor tyrosine kinase family and participates in various signal pathways, including B cell receptor (BCR) pathway. It is well known that BTK plays an important role in the differentiation, activation, proliferation and survival of B lymphocytes.[7-9] Studies in rodent arthritis models have provided evidence for a dual mechanism of action: (i) inhibition of BCR-dependent B lymphocyte activation and autoantibody secretion and (ii) suppression of myeloid cell-dependent inflammatory cytokine production.[10,11]

For over a decade, several BTK inhibitors have been discovered for clinical therapy in hematologic malignancies and chronic inflammatory diseases.[12-15] Among these molecules, Ibrutinib (Figure 1, **1**),[16,17] the most advanced BTK inhibitor, has been approved for B cell malignancies and chronic lymphocytic leukemia.[18-22] Ibrutinib is an

irreversible inhibitor of BTK that covalently binds to Cys481 in the kinase domain. Though covalent BTK inhibitors, such as spebrutinib (CC-292. Figure 1, **2**)[23] and acalabrutinib (ACP-196. Figure 1, **3**),[24,25] are currently involved in clinical development for RA, these molecules actually possess many safety risks. For instance, the Michael receptor portions of covalent inhibitors raise the concern of unwanted off-target inhibition.[26] In addition, haptenization of serum proteins by reactive groups potentially leads to allergic reactions in patients, such as fever, lymphadenopathy, edema and albuminuria. It is widely acknowledged that reversible inhibitors are more likely to provide a lower risk of toxicity in RA patients compared to an irreversible inhibitor. However, compared to covalent inhibitors, the development of reversible BTK inhibitors has been slow.[27-46] To date, no reversible inhibitors have been approved for clinical applications. The well-known noncovalent BTK inhibitors, RN-486 (Figure 1, **4**) and GDC-0834 (Figure 1, **5**), both suffer from poor stability and pharmacokinetic (PK) profiles.[42] Considering the prospects of BTK for the treatment of autoimmune disorders, the development of novel reversible inhibitors with favorable drug-like properties is

urgently needed. In this work, a structure-hopping strategy was applied to discover 4-aminoquinoline-3-carboxamide derivatives as potent BTK inhibitors. Removal of the insignificant nitrogen and incorporation of methoxy and fluorine group substitutions significantly improved the aqueous solubility without compromising the activity against BTK. The most potent inhibitor exhibited strong inhibition of BTK and cellular Tyr223 autophosphorylation. In addition, the modeling of compound **25** in the active site of BTK suggested that the binding pose of our reversible inhibitor was orthogonal to that of Ibrutinib. As a result, **25** exhibited an IC_{50} value of 39 nM against the BTK^{C481S} protein and provided improved kinase selectivity when compared to Ibrutinib, particularly against EGFR, TEC, and ITK.[17,47-49] In a rodent collagen-induced arthritis (CIA) model, compound **25** efficiently reduced paw swelling without a loss in body weight, implying that our inhibitor is efficacious and well tolerated in this study.

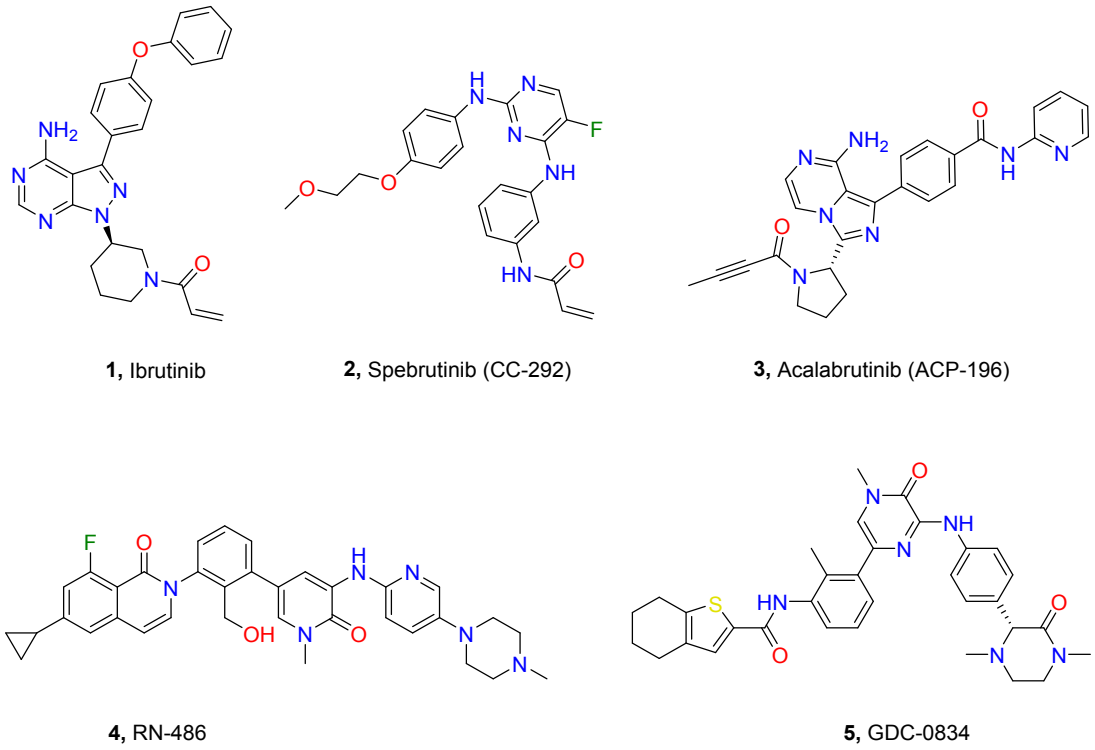

Figure 1. Well-known BTK inhibitors.

RESULTS AND DISCUSSION.

Design and *in vitro* study. Previously, compound **6** was reported as a potent reversible BTK inhibitor.[35] While it demonstrated good *in vitro* activity against BTK, compound **6** exhibited poor aqueous solubility (at pH 7.4 < 0.05 μg/mL), which limited its *in vivo* study. Given the stability and inhibitory activity of compound **6**, we envisioned that optimization might yield a promising lead candidate with improved physiochemical

properties with a retention in potency. It is well acknowledged that compounds with suitable aqueous solubility and CLogP values are more likely to provide acceptable PK properties for oral administration.[50]

Our preliminary studies suggested that the cinnoline moiety might be the source of the poor solubility observed for compound **6**. By analyzing the binding mode of **6** (PDB code: 4Z3V), we found that the cinnoline-N2 atoms did not make direct H-bond interactions with the kinase domain. Based on this observation, the initial design was to remove the insignificant nitrogen and introduce various substitutions, which aimed to disrupt the molecular planarity and lead to additional interactions with the protein.

To our delight, compared to compound **6**, compound **7** bearing a 4-aminoquinoline-3-carboxamide core improved the aqueous solubility by more than 200-fold but with a significant decrease in inhibitory activity. Additionally, compound **7** exhibited a suitable CLogP value, consistent with our drug-like physicochemical criteria. However, replacement of the cinnoline moiety with 4-hydroxyquinoline-3-carboxamide (**8**) resulted

in a dramatic loss in BTK inhibition, indicating that the 4-NH_2 group is important for ligand binding (Table 1).

The docking pose of compound **7** bound to the ATP site of BTK suggested that the 4-aminoquinoline-3-carboxamide moiety would form three direct and one water-mediated H-bond interaction with the hinge region of BTK. The indazole moiety stabilized the conformation of the P-loop by forming crucial hydrogen bonds with Phe413 and Gly414 (Figure 2A). Compared to RN-486, compound **7** lacked the hydrophobic interaction with the H3 pocket of BTK, which induced a significant conformational change in BTK such that the key activating tyrosine, Tyr551, was unphosphorylated and sequestered from solvent (Figure 2B). It has been reported that the H3 pocket is responsible for the exquisite selectivity of the well-known reversible BTK inhibitor CGI-1746.[28] Based on these observations, the first design was to compensate for the hydrophobic interaction with the H3 pocket of the quinoline compounds.

Table 1. *In vitro* BTK inhibition, aqueous solubility and CLogP value

Compd.	Structure	BTK Inhibition (% at 100 nM)[a]	Aq. solubility (μg/mL)[b]	CLogP[c]
6	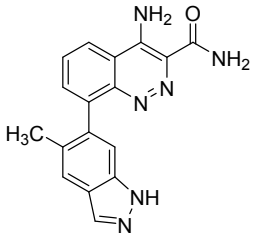	92.1 ± 3.9	<0.05	2.51
7	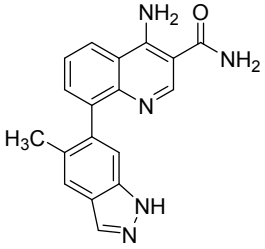	54.2 ± 0.4	10.5	3.07
8	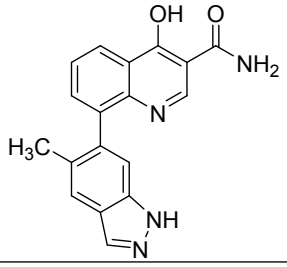	15.5 ± 2.8	n.d.	4.04

a. BTK inhibition (%) by the compound at 100 nM, data represents as mean ± SD of triplicates. b. Kinetic solubility (μg/mL) in PBS (pH 7.4) at 25 °C, determined by HPLC, n=3. c. Values are predicted by ChemBioDraw software Ultra 14.0.

Because the methyl substituent of compound **7** was proposed to have hydrophobic interactions with Leu528, the quinoline and indazole rings were locked at a dihedral angle of 104°. To increase the possibility that the extended groups could approach the

H3 pocket, the methyl group should be removed. As shown in Table 2, compound **9** without the methyl substituent inhibited BTK 41.6% at 100 nM, which was less potent than compound **7**. The hydrophobic phenoxyl, phenylamino, benzyloxyl, and benzyl(methyl)amino groups provided obvious changes in the overall lipophilicity and significantly decreased the inhibitory activity (**10**-**13**). Similarly, the 1,1'-biphenyl-4-yloxyl, 1,1'-biphenyl-3-yloxyl and 4-(4-phenoxyphenoxyl) substituted compounds showed very weak inhibition of BTK kinase (**14**-**16**). We suspected that our designed compounds failed to induce the formation of the H3 pocket; instead, the substituted groups increased the steric bulk and prohibited the inhibitors from accessing to the ATP binding site of BTK.

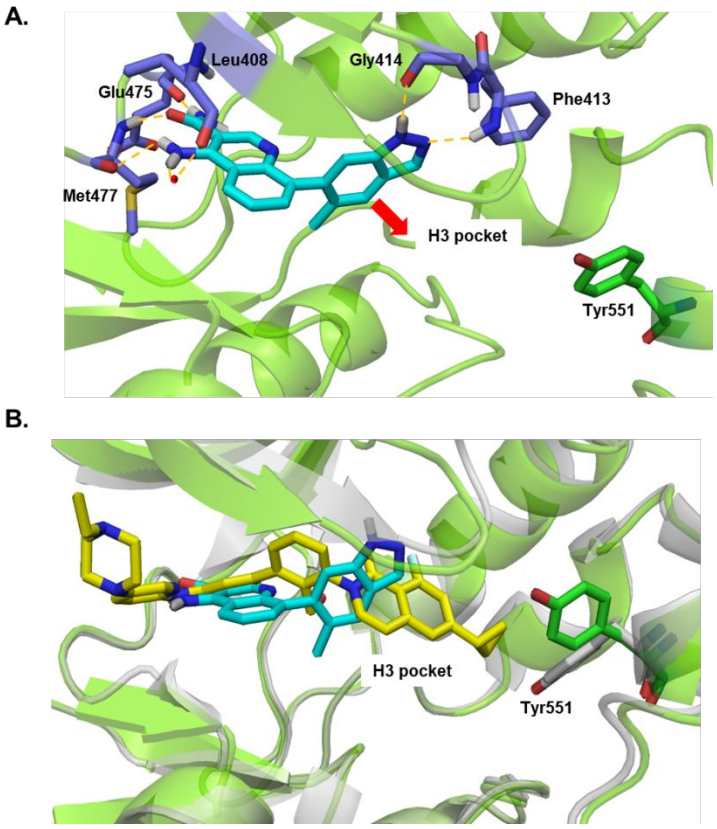

Figure 2. (A) Putative binding mode of compound **7**. The red arrow points out the extended orientation for the hydrophobic groups to grow toward the H3 pocket. Selected residues are displayed in stick representation. Orange dashes represent hydrogen bonds. (B) Docking structure of BTK bound to compound **7** (green and blue) superimposed on X-ray cocrystal structure of BTK bound to RN-486 (PDB code: 4OTR, gray and yellow). RN-486 had hydrophobic interaction with H3 pocket which induced a

significant position change of key activating tyrosine Tyr551 such that it was in the unphosphorylated state and sequestered from solvent.

Table 2. Enzymatic BTK potency of compounds bearing lipophilic groups on the indazole ring

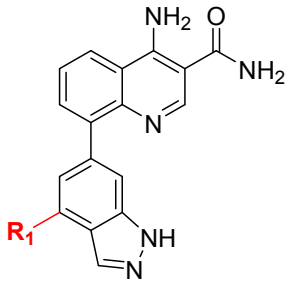

Compd.	R_1	BTK Inhibition (% at 100 nM)[a]	CLogP[b]
9	H	41.6 ± 0.3	2.87
10	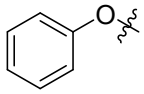	3.9 ± 1.3	4.96
11	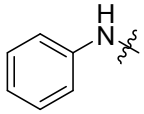	10.4 ± 6.2	4.88
12	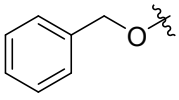	9.5 ± 0.7	4.97
13	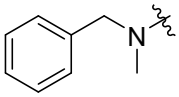	24.7 ± 0.9	5.19
14	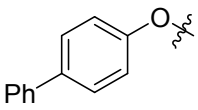	10.7 ± 2.8	6.85

15	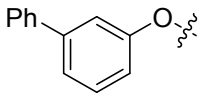	n.a.	6.85
16	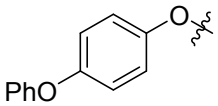	11.8 ± 3.5	7.06

a. BTK inhibition (%) by the compound at 100 nM, data represents as mean ± SD of triplicates. n.a. means no activity. b. Values are predicted by ChemBioDraw software Ultra 14.0

Our second optimization focused on introducing additional interactions with the protein, seeking highly potent inhibitors with a minimal change to the lipophilicity. Quite often, fluorine is used to modulate physicochemical properties, improve metabolic stability, and enhance binding affinity to the target protein.[51] As shown in Table 3, compound **17**, with a 5-F substitution, exhibited a significantly improved effect on BTK, which maintained a substantial amount of the BTK inhibition but potentially increased the aqueous solubility profile relative to **6**. Furthermore, we explored the potency of the compounds with 6-F, 6-NO_2 and 6-NH_2 substitutions (**18**-**20**), but only compound **20** displayed an acceptable inhibition rate of 36.5% inhibition at a concentration of 20 nM. In addition, replacement of the indazole by a benzimidazolone ring resulted in a loss of

affinity for BTK (**21**-**24**), which might be attributed to the missing π-stacking interaction with the P-loop. Finally, we kept the 5-F substitution and replaced the methyl group with a methoxy group on the indazole ring. The resulting compound **25** exhibited 68.7% inhibition at a concentration of 20 nM, which might possess higher potency and more favorable drug-like properties than the lead compound.

Inspired by the improved activity of the 4-aminoquinoline-3-carboxamide derivatives, the selected compounds were further assessed by their IC_{50} values against BTK and kinetic aqueous solubility profiles. As shown in Table 4, the compounds bearing a quinoline core showed over a 100-fold improvement in aqueous solubility, supporting our initial strategy. The 5-F substitution on the quinoline ring exhibited a 6-fold increase in potency (**17**, IC_{50} of 11.6 nM; **7**, IC_{50} of 72.8 nM). Compound **25** was found to be equipotent to compound **6** but with significantly improved aqueous solubility (at pH 7.4 = 7.3 μg/mL), which was more advantageous for further *in vivo* tests.

Table 3. *In vitro* potency of 4-aminoquinoline-3-carboxamide derivatives

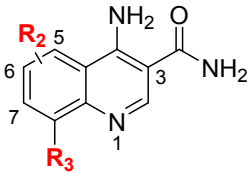

Compd.	R_2	R_3	BTK Inhibition	CLogP[b]
17	5-F	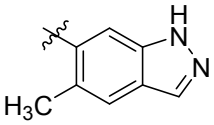	45.9 ± 1.2	3.25
18	6-F	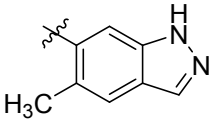	25.3 ± 11.8	3.25
19	6-NO_2	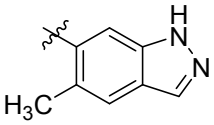	12.8 ± 7.7	2.92
20	6-NH_2	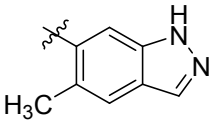	36.5 ± 6.7	2.52
21	5-F	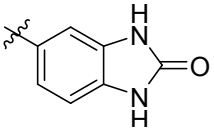	9.3 ± 2.8	2.55
22	6-F	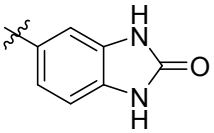	5.1 ± 3.8	2.55
23	5-F	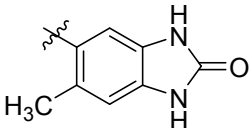	n.a.	2.75
24	6-F	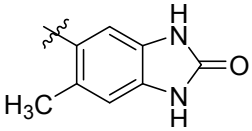	10.0 ± 5.9	2.75
25	5-F	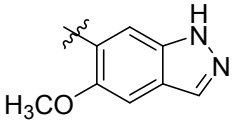	68.7 ± 1.3	2.83
6	-	-	44.6 ± 4.6	2.51

a. BTK inhibition (%) by the compound at 20 nM, data represents as mean ± SD of triplicates. n.a. means no activity. b. Values are predicted by ChemBioDraw software Ultra 14.0.

Table 4. IC_{50} values and aqueous solubility profiles

Compd.	BTK IC_{50} (nM)[a]	Aq. solubility (μg/mL)[b]
7	72.8 ± 0.9	10.5
17	11.6 ± 0.7	5.2
25	5.3 ± 1.3	7.3
6	5.6 ± 1.0	<0.05

a. Data is mean ± SD of three independent experiments. b. Kinetic solubility (μg/mL) in PBS (pH 7.4) at 25 °C, determined by HPLC, n=3.

In the BCR signaling pathway, BTK Tyr551 transphosphorylation is followed by the autophosphorylation of Tyr223 in the SH3 domain. In this way, BTK is activated and transphosphorylates the downstream substrate PLCγ2. Given their good kinase activity, selected compounds were further evaluated for their inhibition of cellular autophosphorylation in Ramos cells. Herein, the phosphorylation levels of BTK (Tyr223) and total BTK protein levels were analyzed by western blotting with anti-pY223 or anti-

total BTK antibodies. As shown in Figure 3A, compounds **6**, **17** and **25** all exhibited dose-dependent inhibition and efficiently blocked Tyr223 autophosphorylation at a concentration of 1 μM. As expected, inhibitor **25** (EC_{50} of 42.7 nM) was 2.4-fold more potent than **6** (EC_{50} of 100.9 nM) in cell-based assays (Figure 3B), which may be derived from the better aqueous solubility and cell permeability of the quinoline core.

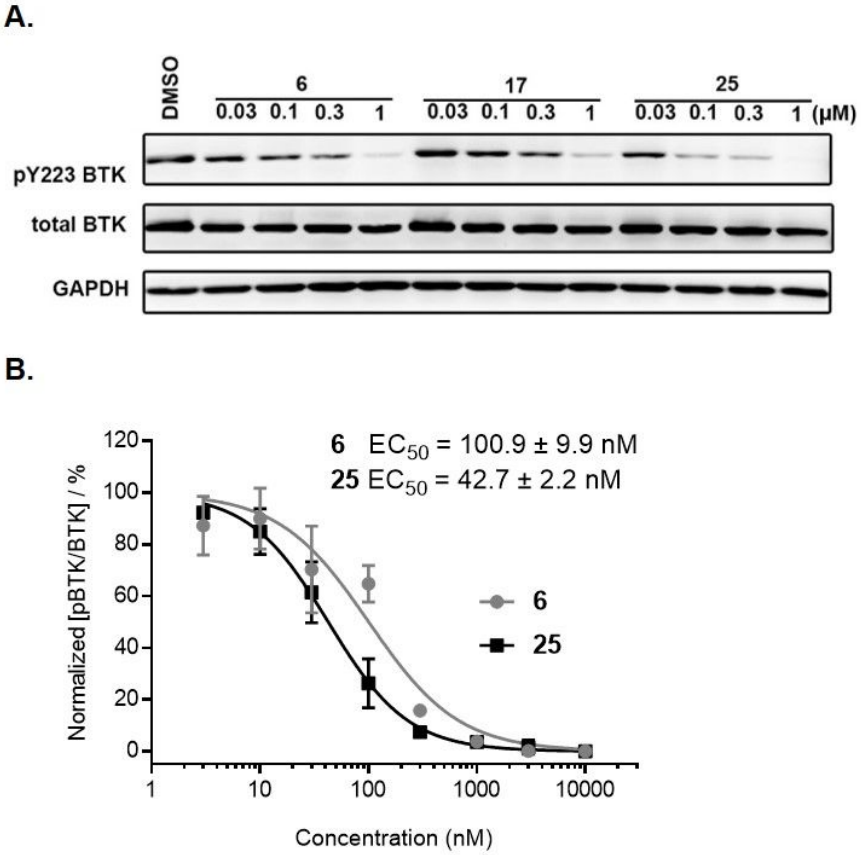

Figure 3. BTK inhibitors blocked autophosphorylation of Tyr223. (A) Concentration-dependent inhibition by compound **6**, **17**, **25** in Ramos cells of pervanadate mediated phosphorylation of BTK Tyr223. The phosphorylation levels of BTK (Tyr223) and total BTK protein levels were analyzed by western blotting. (B) EC_{50} curves of compound **25** and **6**. Data is mean ± SD of three independent experiments.

Docking study and selectivity profile. To better understand why the substitution of fluorine and methoxy groups resulted in more than a 10-fold improvement in potency compared to compound **7** (**7**, IC_{50} = 72.8 nM; **25**, IC_{50} = 5.3 nM), we performed molecular docking studies on compounds **7** and **25**. As shown in Figure 4A, when properly aligned, compound **25** appeared to situate into a space that was slightly different from that of **7**. The incorporation of the fluorine and methoxy substitutions likely tuned the conformation, altering the dihedral angle between the quinoline and indazole rings from 104° in compound **7** to 100° in compound **25**. In addition, the fluorine atom was proposed to add a hydrophobic interaction with Leu528. The movement of the indazole ring allowed **25** to form stable π–cation interactions with Lys430 (Figure 4B).

The modeling of our inhibitors in the active site of BTK also suggested that the binding pose of compound **25** was orthogonal to that of Ibrutinib (Figure 5A). Compound **25** did not interact with Cys481 that was responsible for the covalent interaction of Ibrutinib. Given that the BTK^{C481S} mutation is prevalent in patients who relapse after Ibrutinib treatment, we hypothesized that our inhibitor could retain activity against the C481S mutant form of BTK. Herein, ACP-196 was selected as a control compound, which is a second-generation covalent inhibitor of BTK, with higher potency and less off-target effects than Ibrutinib. As expected, **25** efficiently inhibited BTK^{C481S} with an IC_{50} value of 39 nM. In contrast, ACP-196 only showed equivalent potency to **25** against BTK^{WT} but failed to block the phosphorylation effect of BTK^{C481S}. In addition, we tested the effects of **25** and ACP-196 against EGFR and TEC, two well-known off-targets of Ibrutinib. To our delight, **25** and ACP-196 had no effect on EGFR, and their IC_{50} values were above 2 μM. For TEC kinase, **25** was less potent than ACP-196. The selectivity of **25** for BTK^{WT} over TEC was more than 40-fold (Figure 5B). Inspired by the preliminary selectivity data, a kinase selectivity profile for compound **25** was further assessed for

the closely related kinases from the TEC and SRC families (Table 5). Based on the determined IC_{50} values, compound **25** was more selective for BTK than other members of the TEC and SRC kinase families. The selectivity ratios were all greater than 30-fold, except for BLK (28-fold). It is of note that compound **25** was 58-fold less potent against ITK, which is highly homologous to BTK but positively regulates the T cell receptor signaling pathway and acts as a crucial regulator in multiple physiological processes of T lymphocytes.[52] The selectivity data indicated that **25** might have a slight effect on the physiological process of T cells. Above all, it was envisioned that our reversible inhibitor would have fewer side effects than the covalent BTK inhibitors. Because **25** could have a profile to provide potential treatment for patients with B cell malignancies harboring the BTK^{C481S} mutation with less off-target effects, this compound is currently being evaluated in Ibrutinib-resistant NHL and CLL studies.

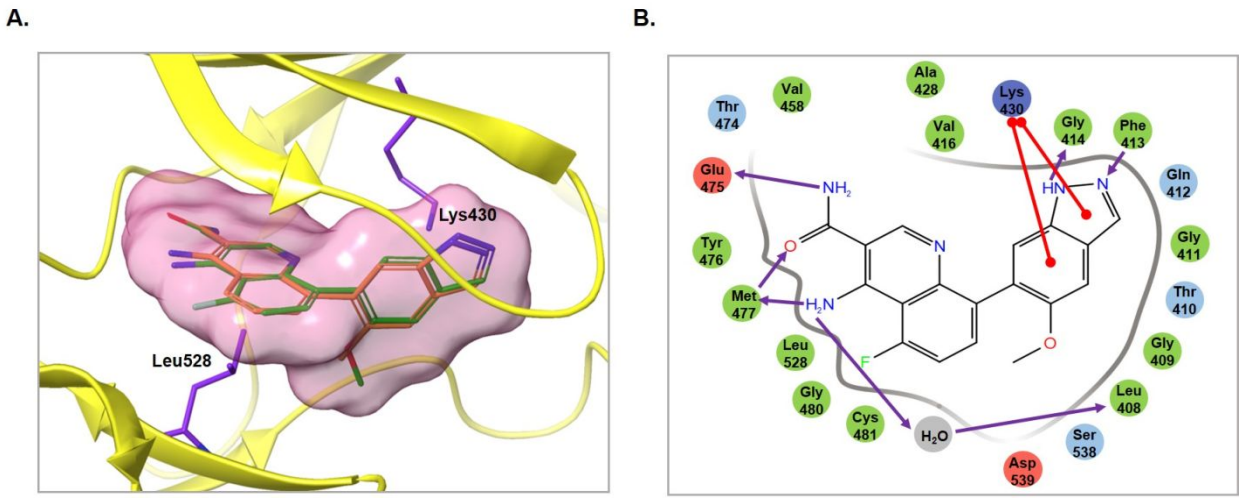

Figure 4. Docking study of 4-aminoquinoline-3-carboxamide derivatives. (A) Putative binding modes of compound **7** (orange) and **25** (green) in the BTK kinase domain (yellow cartoon). Selected residues are shown in stick representation. (B) Summary of receptor interactions with compound **25**. Dark blue ball (positive charged interaction); cyan and red ball (polar interaction); green ball (hydrophobic interaction); purple arrow (H-bond); red line (π–cation interaction).

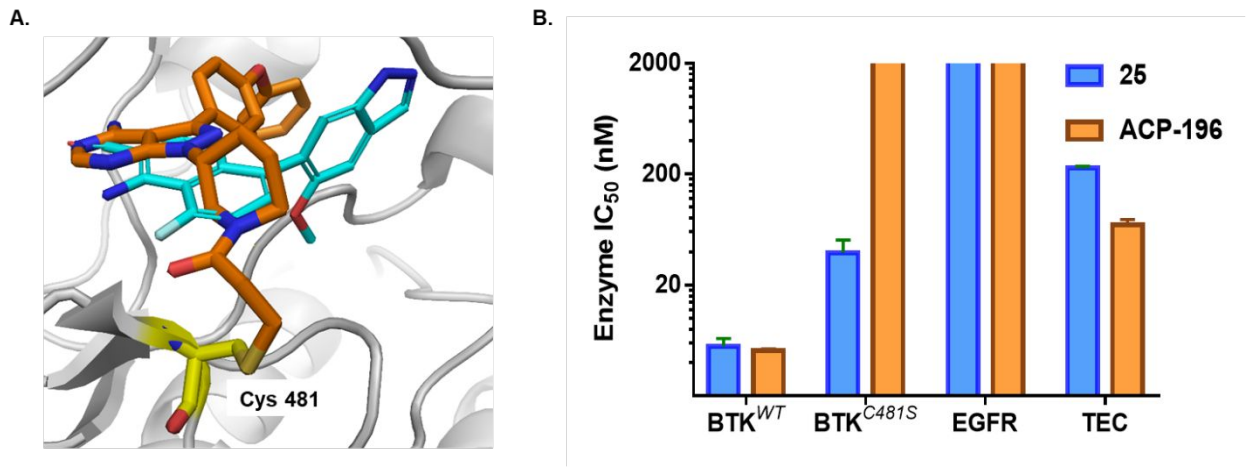

Figure 5. Compound **25** binds to the kinase domain of BTK with a different manner of the existing ATP-mimetic covalent inhibitors. (A) Superposition of the cocrystal structure of Ibrutinib (orange, PDB code: 5P9J) and docking pose of **25** (blue). Ibrutinib forms a covalent bond with residue Cys481 and occupies the hydrophobic pocket behind the gatekeeper residue Thr474, **25** does neither. Residue Cys481 is shown in stick representation. (B) IC_{50} values of **25** and ACP-196 against BTK, BTK^{C481S}, EGFR and TEC kinases.

Table 5. Kinase selectivity profile of compound **25**

Kinase	Kinase family	IC_{50} (nM)[a]	Selectivity ratio[b]
BTK	TEC	5.3	/
ITK	TEC	306.9	58

TEC	TEC	227.0	43
BLK	SRC	150.2	28
SRC	SRC	902.5	170
FYN	SRC	165.2	31
YES	SRC	>10000	>1000

a. Run in triplicates. b. Kinase of interest IC_{50}/BTK IC_{50}.

Plasma stability and *in vivo* PK profile. Inspired by the high potency and selectivity profile, we further evaluated the drug-like properties of compound **25** with a plasma incubation assay and a rat pharmacokinetic study. Determination of the plasma recovery rate revealed the remarkable stability of our BTK inhibitor. The percent of the remaining parent compound was above 88% after incubation in plasma samples from humans, dogs, rats, mice and monkeys at 37°C for up to 2 h. In addition, no significant interspecies differences were observed (Table 6). Compound **25** also exhibited a favorable PK profile in rats. After a single 2 mg/kg iv dose, the mean clearance rate (CL) and half-life ($t_{1/2}$) of compound **25** were 20.8 mL/min/kg and 1.2 h, respectively. Meanwhile, acceptable absorption properties were demonstrated after oral administration at a dose of 5 mg/kg. Compound **25** showed a moderate oral bioavailability (*F*) of 25% (Table 7).

Table 6. *In vitro* plasma stability of compound **25**[a]

Compd.	Human (%)	Dog (%)	Rat (%)	Mouse (%)	Monkey (%)
25	93%	88%	96%	98%	88%

a. % of remaining parent compound after 2 h incubation in plasma at 37 °C with initial concentration of 1 μM.

Table 7. Pharmacokinetic profile of compound **25** in rat[a]

Compd.	CL (mL/min/kg), iv	V_d (L/kg)	$T_{1/2}$ (h), iv	F (%)
25	20.8	2.1	1.2	25

a. Male Sprague-Dawley rats iv at 2 mg/kg (10% DMSO, 90% PEG400) and po at 5 mg/kg (0.5% methylcellulose suspension), n=6.

***In vivo* CIA study.** Given the high *in vitro* potency and favorable PK profile of compound **25**, we further evaluated the potential of our reversible inhibitor to treat RA using a rodent collagen-induced arthritis (CIA) model. Arthritis was established in male DBA/1 mice by injecting type II collagen twice separately on day 0 and day 20 of the study. On

day 29, the CIA model mice were randomized and treated orally with 0.2 mg/kg dexamethasone (DXMS), 10 mg/kg compound **25** or vehicle control QD. The paw volumes were then measured on days 29, 33, 36, 40, and 43. From day 29 to day 36, in vehicle-treated mice, there was a dramatic increase in the paw volume, indicating that the arthritis model was successfully established. Compared to the vehicle group, the mice that were administered **25** or DXMS did not show disease progression. Furthermore, the paw volumes of the drug-treated groups significantly decreased over the duration of treatment. The QD 10 mg/kg dosage of **25** showed comparable efficacy relative to DXMS (Figure 6A). During the study period, the body weights of the mice in these four groups were recorded to evaluate the toxicity of the test compounds. As shown in Figure 6B, the mice in the **25**-treated group had a better appetite than those treated with DXMS, which implied that our inhibitor may have lower side effects *in vivo*.

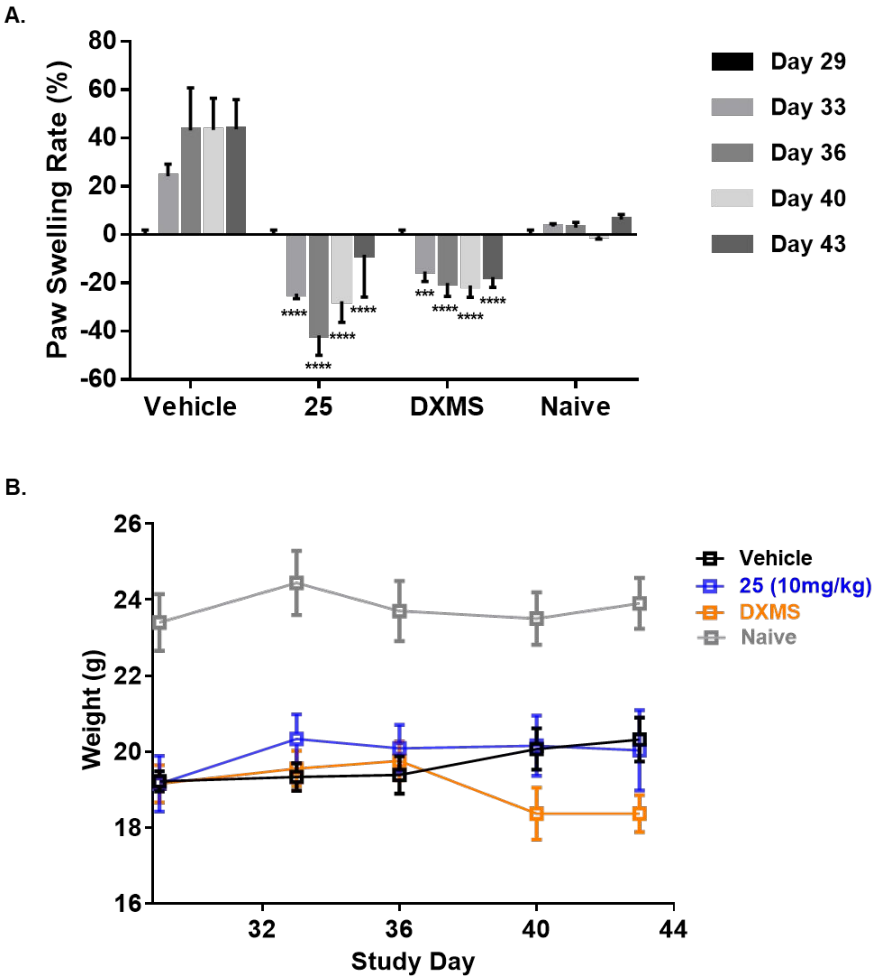

Figure 6. Efficacy of compound **25** in rodent CIA model. (A) The paw swelling rate of four groups, including vehicle, **25** (10 mg/kg, QD), DXMS (0.2 mg/kg, QD) and naive, male DBA/1 mice, n=6. Data represent as mean ± SEM in the graphs. $^{***}P < 0.001$, $^{****}P < 0.0001$ *vs* vehicle control by Dunnett's test. (B) The average body weights of the mice over study days.

Chemistry. All of the title molecules **7**-**25** were prepared with a convergent route as depicted in Schemes 1-4. Scheme 1 shows the preparation of the quinoline moieties, intermediates **30a**-**d**. The corresponding anilines and diethyl ethoxymethylenemalonate were heated at 100°C for 2 h. After completion of the reaction, the mixtures were added into boiling DOWTHERM A. Cyclization was accomplished under high temperatures to give quinolones **27a**-**d**. After hydrolysis, one-pot reactions by the addition of $SOCl_2$ followed by ammonium solution furnished compounds **29a**-**d**. Then, intermediates **30a**-**d** were finally accomplished by treating **29a**-**d** with 7 M NH_3 in MeOH. Notably, the products that resulted from these four steps were purified by filtration without column chromatography, simplifying and expediting the synthesis.

Scheme 1. Synthesis of quinoline intermediates[a]

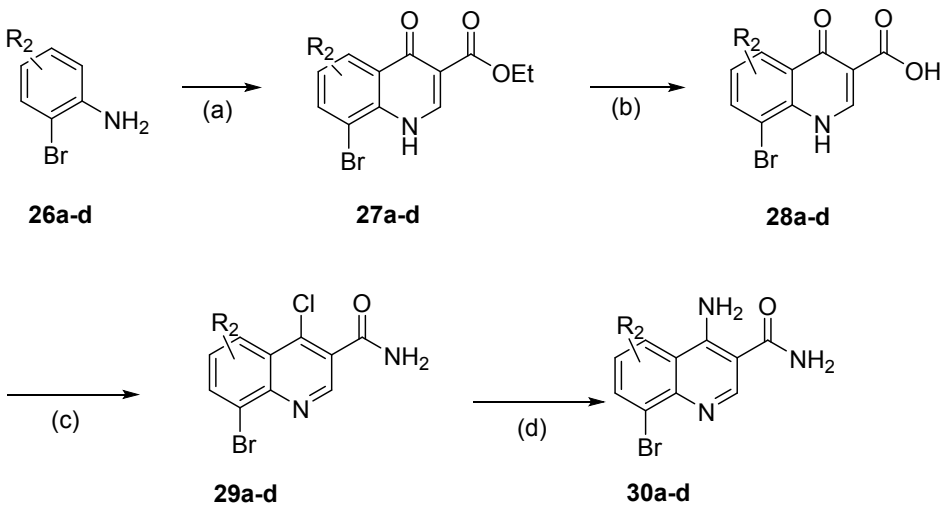

[a]Reagents and conditions: (a) (i) diethyl ethoxymethylenemalonate, 100 °C, 2 h, (ii) Dowtherm A, 250 °C, 4-12 h, 40-60% (b) LiOH, THF/EtOH/H_2O= 4:4:2, 55 °C, 4-8 h, 75-82%; (c) (i) $SOCl_2$, DMF, 70 °C, 3-6 h, (ii) $NH_3 \cdot H_2O$, DCM, 0 °C - rt, 1 h, 40-60%; (d) 7M NH_3 in MeOH, 80 °C, overnight, 50-55%.

The synthesis of title compounds **9**-**16** is shown in Scheme 2. Starting from 1-bromo-3,5-difluorobenzene **31**, after treatment with LDA and DMF, the aldehyde intermediate **32** was obtained. Then the intermediates **33b**-**h** were furnished by an SN_{AR} reaction and converted into indazoles via the addition of hydrazinehydrate. Specifically, the synthesis of compound **9** was started from the commercially available 4-bromo-2-fluorobenzaldehyde **33a**. Under strongly basic conditions, the brominated indazoles were transformed into their corresponding borate intermediates **35a**-**h**. The final step was a Suzuki couplings, which worked well under microwave conditions.

Scheme 2. Synthetic route of title compounds **9-16**[a]

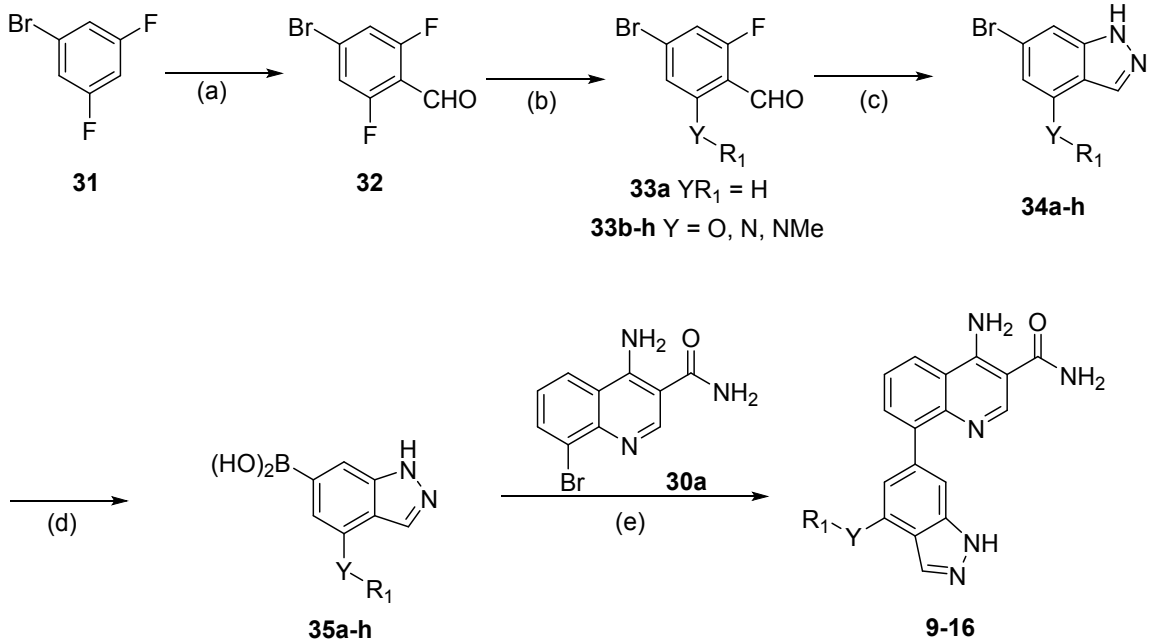

[a]Reagents and conditions: (a) diisopropylamine, *n*-butyllithium, DMF, anhydrous THF, -78°C-rt, 3 h, 50%; (b) R_1YH, K_2CO_3, DMA, 100°C, 3-8 h, 35%-61%; (c) $N_2H_4 \cdot H_2O$/DME 1:1, 170-200°C, 24-48 h, 20-62%; (d) *t*-buLi, tributyl borate, anhydrous THF, -78 °C- rt, overnight, 21-62%; (e) Pd(dppf)Cl_2, 2M Na_2CO_3, 1,4-dioxane, microwave, 140 °C, 1-2 h, 23-84%.

As shown in Scheme 3, the compounds bearing methyl- or methoxyl-substituted indazoles were prepared according to the described synthetic methods. First, the reduction of **36** gave the substituted aniline intermediates **37a-b**. In this synthetic route, milder conditions devoid of high temperatures and strong bases were used to prepare the indazole intermediates. Initially, the anilines were transformed into diazonium salts

by the addition of fluoroboric acid and $NaNO_2$. Then, under KOAc conditions, the cyclization occurred to afford the 5-membered indazole rings. The NH groups were protected with a Boc group with DMAP and Et_3N. After Miyaura borylation, Boc deprotection was accomplished in the presence of TFA. Finally, a Suzuki coupling reaction was used to furnish the desired compounds **7**, **25** and **17-20**.

Scheme 3. Synthetic route of title compounds **7**, **25** and **17-20**[a]

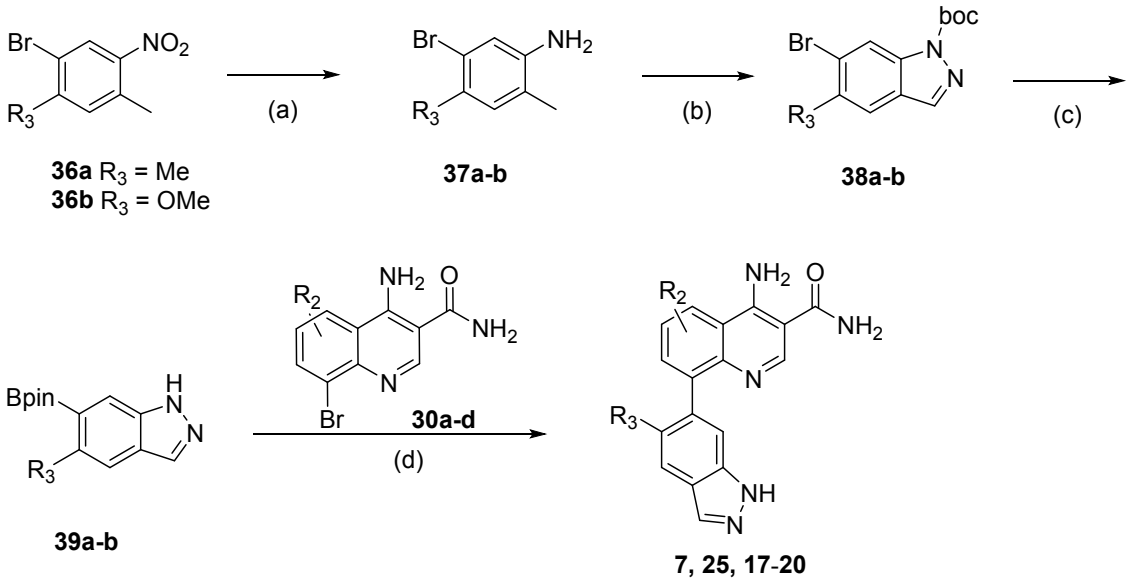

[a]Reagents and conditions: (a) Fe, NH_4Cl, EtOH/H_2O 3:1, 80°C, 1 h, 80-90%; (b) (i) 50% HBF_4, $NaNO_2$, H_2O, 0°C, 3 h; (ii) AcOK, 18-crown-6, $CHCl_3$, rt, 3 h; (iii) Boc_2O, DMAP, Et_3N, MeCN, rt, 1 h, 25-35%; (c) (i) Pd(dppf)Cl_2, B_2pin_2, KOAc, 1,4-dioxane, 90°C, overnight; (ii) TFA/DCM 1:1, rt, 2 h, 55-60%; (d) Pd(dppf)Cl_2, 2M Na_2CO_3, 1,4-dioxane, 140°C, microwave, 1-2 h, 44-65%.

Title compounds **21-24** were synthesized as shown in Scheme 4. Cyclization of **40** with CDI in DMF at room temperature produced the benzimidazolones in of 75% and 78% yield. Miyaura borylation was performed as mentioned above. Additionally, Suzuki coupling reactions were conducted to obtain the desired compounds.

Scheme 4. Synthetic route of title compounds **21-24**[a]

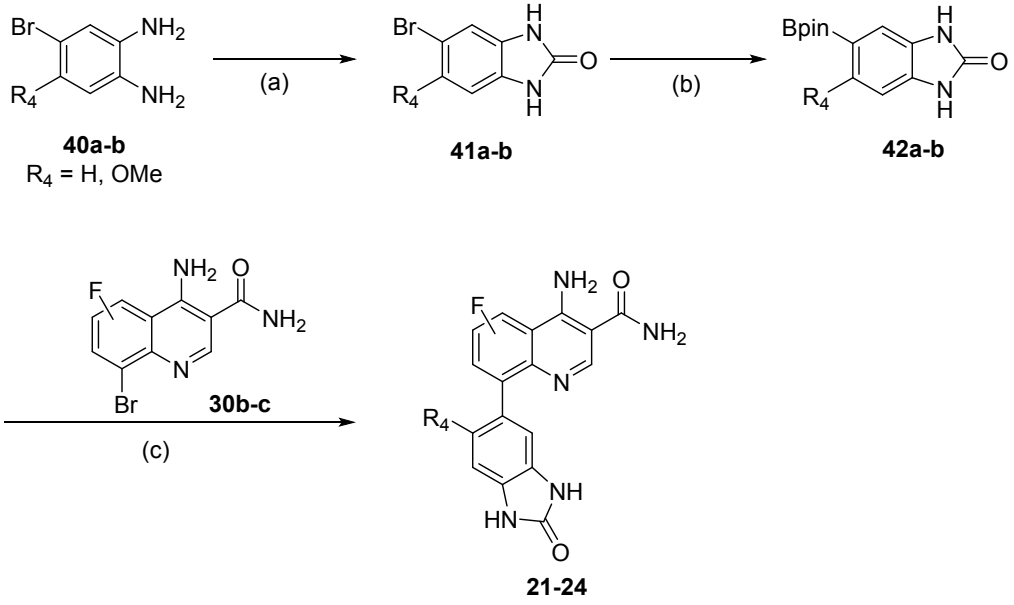

[a]Reagents and conditions: (a) *N, N'*-carbonyldiimidazole, rt, overnight, 75-78%; (b) $Pd(dppf)Cl_2$, B_2pin_2, KOAc, 1,4-dioxane, 90°C, 6 h, 80-83%; (c) $Pd(dppf)Cl_2$, 2M Na_2CO_3, 1,4-dioxane, microwave, 140°C, 2 h, 43%-51%.

CONCLUSION.

In summary, we have disclosed a series of novel 4-aminoquinoline-3-carboxamide derivatives as potent reversible BTK inhibitors with significantly improved drug-like properties, especially the aqueous solubility profile. Compound **25** exhibited high potency with an enzymatic IC_{50} value of 5.3 nM against BTK and a cellular autophosphorylation inhibition EC_{50} of 42.7 nM. As supported by docking studies, the incorporation of fluorine and methoxy substitutions resulted in a more than 10-fold increase in potency through the introduction of additional interactions (a hydrophobic interaction with Leu528 and π–cation interaction with Lys430) and likely tuned the bound conformation. In addition, our inhibitors are predicted to bind to the kinase domain of BTK in an orthogonal orientation to that of Ibrutinib, providing improved selectivity over the closely related TEC and SRC family kinases. In the rodent CIA model, representative compound **25** efficiently reduced paw swelling without affecting the appetite of the mice, which implied that our inhibitor was both efficacious and well tolerated in this study. Furthermore, a plasma recovery assay and a rat pharmacokinetic

study demonstrated the favorable PK profile of our compound. Above all, compound **25** has been identified as a novel and highly potent reversible inhibitor that has the potential to behave as an orally available therapy for the treatment of rheumatoid arthritis.

EXPERIMENTAL SECTION

Materials. All commercial materials purchased from Bidepharm, Aladdin and J&K Chemical LTD were used without further purification. All solvents we used for reaction and purification were analytical grade. Analytical TLC was performed on Yantai Chemical Industry Research Institute silica gel 60 F254 plates and flash column chromatography was performed on Qingdao Haiyang Chemical Co. Ltd silica gel 60 (200-250 mesh). The rotavapor was BUCHI's Rotavapor R-3. MicroCal iTC200 system (GE Healthcare). The ^{1}H, ^{13}C, ^{19}F NMR spectra were recorded on a Bruker 400 MHz spectrometer. Low-resolution mass spectral analyses were performed with a Waters AQUITY UPLCTM/MS. Purity of all title compounds was ≥ 95% pure. HPLC purity determination was performed on a SHIMADZU system using a Vydac 218TP C18

column (5 μm, 4.6 × 250 mm) with a gradient of 9%-80% acetonitrile (containing 0.1% TFA) in water (containing 0.1% TFA) over 20 min. UV detection (λ = 254 nm). ACP-196 was purchased from MedChemExpress (HY-17600-32534), the purity was above 99%. Dexamethasone was purchased from MedChemExpress (HY-14648-11202), the purity was above 98%.

General procedure for the synthesis of title compounds 7-25.

To a mixture of 4-amino-8-bromoquinoline-3-carboxamide **30a-d** (0.1 mmol), 2M aqueous $NaHCO_3$ (0.1 mL) and $Pd(dppf)Cl_2$ (7 mg, 0.01 mmol) in 1, 4-dioxane (2 mL) was added boronic acid intermediates **35a-h** (0.15 mmol) or borates **39a-b** (0.15 mmol) or **42a-b** (0.15 mmol) and heated in microwave at 140 °C for 1-2 h. The catalyst was removed by filtration and the filtrate was evaporated to dryness. Purification by column chromatography on silica gel (eluting with DCM-MeOH, 10:1) afforded the title compounds **7-25**

4-amino-8-(5-methyl-1H-indazol-6-yl)quinoline-3-carboxamide (7). White solid. Yield: 44%. ^{1}H NMR (400MHz, CD_3OD, ppm) δ 8.60 (s, 1H), 8.36 (d, J = 7.3 Hz, 1H), 8.05 (s,

1H), 7.73-7.67 (m, 3H), 7.43 (s, 1H), 2.02 (s, 3H). LRMS (ESI) calcd for $C_{18}H_{15}N_5O$ $[M+H]^+$: 318.36, found 318.70. HPLC purity: 95%. t_R = 12.12 min.

4-hydroxy-8-(5-methyl-1H-indazol-6-yl)quinoline-3-carboxamide (8). White solid. Yield: 56%. ^1H NMR (400MHz, DMSO-d_6, ppm) δ 13.14 (s, 1H), 9.30 (s, 1H), 8.47 (s, 1H), 8.34 (d, J = 7.6 Hz, 1H), 8.11 (s, 1H), 7.79 (s, 1H), 7.63-7.46 (m, 4H), 2.02 (s, 3H). LRMS (ESI) calcd for $C_{18}H_{14}N_4O_2$ $[M+H]^+$: 319.34, found 319.58.

4-amino-8-(1H-indazol-6-yl)quinoline-3-carboxamide (9). White solid. Yield: 40%. ^1H NMR (400MHz, CD_3OD, ppm) δ 8.67 (s, 1H), 8.35 (d, J = 8.5 Hz, 1H), 8.14 (s, 1H), 7.91 (d, J = 8.3 Hz, 1H), 7.84 (d, J = 7.1 Hz, 1H), 7.72-7.68 (m, 2H), 7.29 (d, J = 8.3 Hz, 1H). LRMS (ESI) calcd for $C_{17}H_{13}N_5O$ $[M+H]^+$: 304.33, found 304.54.

4-amino-8-(4-phenoxy-1H-indazol-6-yl)quinoline-3-carboxamide (10). White solid. Yield: 84%. ^1H NMR (400MHz, CD_3OD, ppm) δ 8.67 (s, 1H), 8.21 (d, J = 8.3 Hz, 1H), 7.79 (s, 1H), 7.72 (d, J = 7.1 Hz, 1H), 7.55 (t, J = 7.7 Hz, 1H), 7.41-7.36 (m, 3H), 7.20-7.13 (m, 3H), 6.75 (s, 1H). LRMS (ESI) calcd for $C_{23}H_{17}N_5O_2$ $[M+H]^+$: 396.43, found 396.51.

4-amino-8-(4-(phenylamino)-1H-indazol-6-yl)quinoline-3-carboxamide (11). Yellow solid. Yield: 61%. ^{1}H NMR (400MHz, CD_3OD, ppm) δ 8.68 (s, 1H), 8.20 (d, J = 8.2 Hz, 1H), 8.13 (s, 1H), 7.73 (d, J = 7.0 Hz, 1H), 7.55 (t, J = 7.8 Hz, 1H), 7.25-7.22 (m, 4H), 7.12 (s, 1H), 7.02 (s, 1H), 6.89 (t, J = 7.0 Hz, 1H). LRMS (ESI) calcd for $C_{23}H_{18}N_6O$ $[M+H]^+$: 395.45, found 395.56.

4-amino-8-(4-(benzyloxy)-1H-indazol-6-yl)quinoline-3-carboxamide (12). White solid. Yield: 23%. ^{1}H NMR (400MHz, DMSO-d_6, ppm) δ 13.22 (s, 1H), 8.73 (s, 1H), 8.47 (s, 1H), 8.15 (s, 1H), 7.84 (s, 1H), 7.67 (s, 1H), 7.52 (d, J = 7.1 Hz, 2H), 7.42 (t, J = 7.1 Hz, 2H), 7.35 (t, J = 7.3 Hz, 1H), 7.28 (s, 1H), 6.83 (s, 1H), 5.29 (s, 2H). LRMS (ESI) calcd for $C_{24}H_{19}N_5O_2$ $[M+H]^+$: 410.46, found 410.76.

4-amino-8-(4-(benzyl(methyl)amino)-1H-indazol-6-yl)quinoline-3-carboxamide (13). Yellow solid. Yield: 50%. ^{1}H NMR (400MHz, CD_3OD, ppm) δ 8.63 (s, 1H), 8.32 (d, J = 7.6 Hz, 1H), 8.00 (s, 1H), 7.83 (d, J = 7.6 Hz, 1H), 7.67 (t, J = 8.3 Hz, 1H), 7.35-7.26 (m, 5H), 7.01 (s, 1H), 6.41 (s, 1H), 4.79 (s, 2H), 3.13 (s, 3H). LRMS (ESI) calcd for $C_{25}H_{22}N_6O$ $[M+H]^+$: 423.50, found 423.77.

8-(4-([1,1'-biphenyl]-4-yloxy)-1H-indazol-6-yl)-4-aminoquinoline-3-carboxamide (14). White solid. Yield: 38%. ^{1}H NMR (400MHz, DMSO-d_6, ppm) δ 13.31 (s, 1H), 8.82 (s, 1H), 8.58 (s, 1H), 8.32 (d, J = 8.5 Hz, 1H), 8.02 (s, 1H), 7.87 (s, 1H), 7.77-7.64 (m, 5H), 7.55-7.25 (m, 8H), 6.91 (s, 1H). LRMS (ESI) calcd for $C_{29}H_{21}N_5O_2$ $[M+H]^+$: 472.53, found 472.60.

8-(4-([1,1'-biphenyl]-3-yloxy)-1H-indazol-6-yl)-4-aminoquinoline-3-carboxamide (15). White solid. Yield: 38%. ^{1}H NMR (400MHz, DMSO-d_6, ppm) δ 13.25 (s, 1H), 8.77 (s, 1H), 8.62 (s, 1H), 8.33 (s, 1H), 7.95-7.87 (m, 2H), 7.67-7.65 (m, 3H), 7.51-7.37 (m, 10H), 7.19 (s, 1H), 6.89 (s, 1H). LRMS (ESI) calcd for $C_{29}H_{21}N_5O_2$ $[M+H]^+$: 472.53, found 472.61.

4-amino-8-(4-(4-phenoxyphenoxy)-1H-indazol-6-yl)quinoline-3-carboxamide (16). White solid. Yield: 23%. ^{1}H NMR (400MHz, CD_3OD, ppm) δ 8.65 (s, 1H), 8.34 (d, J = 8.3 Hz, 1H), 7.91 (s, 1H), 7.82 (d, J = 7.1 Hz, 1H), 7.68 (t, J = 8.0 Hz, 1H), 7.39 (s, 1H), 7.32 (d, J = 7.7 Hz, 2H), 7.20 (d, J = 8.8 Hz, 2H), 7.09 (t, J = 7.4 Hz, 1H), 7.02 (d, J =

8.9 Hz, 2H), 6.97 (d, J = 8.2 Hz, 2H), 6.65 (s, 1H). LRMS (ESI) calcd for $C_{29}H_{21}N_5O_3$ $[M+H]^+$: 488.53, found 488.85.

4-amino-5-fluoro-8-(5-methyl-1H-indazol-6-yl)quinoline-3-carboxamide (17). White solid. Yield: 65%. ^{1}H NMR (400MHz, DMSO-d_6, ppm) δ 12.90 (s, 1H), 8.66 (s, 1H), 8.00 (s, 2H), 7.58-7.53 (m, 2H), 7.34-7.29 (m, 2H), 7.23 (s, 1H), 1.96 (s, 3H). ^{13}C NMR (100MHz, DMSO-d_6, ppm) δ 170.5, 159.5 (d, J = 252 Hz), 152.5, 150.3, 148.6, 139.1, 138.7, 137.3 (d, J = 4 Hz), 132.7, 131.3 (d, J = 10 Hz), 129.2, 122.5, 119.4, 110.8, 109.6 (d, J = 22 Hz), 108.5 (d, J = 7 Hz), 103.3, 20.3. ^{19}F NMR (376MHz, DMSO-d_6, ppm) δ -112.8. LRMS (ESI) calcd for $C_{18}H_{14}FN_5O$ $[M+H]^+$: 336.35, found 336.18. HPLC purity: 99%. t_R = 11.57 min.

4-amino-6-fluoro-8-(5-methyl-1H-indazol-6-yl)quinoline-3-carboxamide (18). White solid. Yield: 53%. ^{1}H NMR (400MHz, DMSO-d_6, ppm) δ 12.94 (s, 1H), 8.65 (s, 1H), 8.47 (s, 2H), 8.20 (dd, J = 10.6, 2.6 Hz, 1H), 8.02 (s, 1H), 7.97 (s. 1H), 7.59 (s. 1H), 7.51 (dd, J = 8.6, 2.5 Hz, 1H), 7.34 (s, 1H), 7.29 (s, 1H), 1.98 (s, 1H). LRMS (ESI) calcd for $C_{18}H_{14}FN_5O$ $[M+H]^+$: 336.35, found 336.56.

4-amino-8-(5-methyl-1H-indazol-6-yl)-6-nitroquinoline-3-carboxamide (19). White solid. Yield: 55%. ^{1}H NMR (400MHz, DMSO-d_6, ppm) δ 13.00 (s, 1H), 9.49 (d, J = 2.4 Hz, 1H), 9.06 (s, 2H), 8.80 (s, 1H), 8.22 (d, J = 2.4 Hz, 1H), 8.09 (s, 1H), 8.04 (s, 1H), 7.62 (s, 1H), 7.50 (s, 1H), 7.34 (s, 1H), 2.00 (s, 3H). LRMS (ESI) calcd for $C_{18}H_{14}N_6O_3$ $[M+H]^+$:363.36, found 363.54.

4,6-diamino-8-(5-methyl-1H-indazol-6-yl)quinoline-3-carboxamide (20). To a suspension of 4-amino-8-(5-methyl-1*H*-indazol-6-yl)-6-nitroquinoline-3-carboxamide **19** (26 mg, 0.07 mmol) and NH_4Cl (2.6 mg, 0.05 mmol) in ethanol (0.9 mL) and water (0.3 mL) was added iron powder (23.5 mg, 0.42 mmol). The reaction mixture was heated at 80 ^{o}C for 2 h. The iron was removed by filtration and the filtrated was concentrated to dryness. Purification by column chromatography on silica gel (10% methanol in DCM) afforded **20** (12 mg, 50% yield). ^{1}H NMR (400MHz, DMSO-d_6, ppm) δ 12.88 (s, 1H), 8.37 (s, 1H), 8.02-8.00 (m, 3H), 7.81 (s, 1H), 7.55 (s, 1H), 7.22-7.15 (m, 3H), 6.98 (d, J = 2.3 Hz, 1H), 5.38 (s, 2H), 1.99 (s, 3H). LRMS (ESI) calcd for $C_{18}H_{16}N_6O$ $[M+H]^+$:333.37, found 333.37.

4-amino-5-fluoro-8-(2-oxo-2,3-dihydro-1H-benzo[d]imidazol-5-yl)quinoline-3-carboxamide (21). White solid. Yield: 46%. ^{1}H NMR (400MHz, DMSO-d_6, ppm) δ10.63 (s, 1H), 10.61 (s, 1H), 8.77 (s, 1H), 8.05 (s, 2H), 7.61 (dd, J = 7.8, 6.6 Hz, 1H), 7.40 (s, 2H), 7.28 (dd, J = 13.3, 8.0 Hz, 1H), 7.12 (s, 1H), 7.06 (d, J = 7.9 Hz, 1H), 6.97 (d, J = 8.0 Hz, 1H). LRMS (ESI) calcd for $C_{17}H_{12}FN_5O_2$ $[M+H]^+$: 338.32, found 338.37.

4-amino-6-fluoro-8-(2-oxo-2,3-dihydro-1H-benzo[d]imidazol-5-yl)quinoline-3-carboxamide (22). White solid. Yield: 43%. ^{1}H NMR (400MHz, DMSO-d_6, ppm) δ10.69 (s, 1H), 10.66 (s, 1H), 8.78 (s, 1H), 8.46 (s, 2H), 8.10 (dd, J = 10.6, 2.6 Hz, 1H), 8.04 (s, 1H), 7.55 (dd, J = 9.2, 2.6 Hz, 1H), 7.47 (s, 1H), 7.24 (s, 1H), 7.17 (d, J = 8.0 Hz, 1H), 7.00 (d, J = 8.0 Hz, 1H). LRMS (ESI) calcd for $C_{17}H_{12}FN_5O_2$ $[M+H]^+$: 338.32, found 338.46.

4-amino-5-fluoro-8-(6-methyl-2-oxo-2,3-dihydro-1H-benzo[d]imidazol-5-yl)quinoline-3-carboxamide (23). White solid. Yield: 51%. ^{1}H NMR (400MHz, DMSO-d_6, ppm) δ10.51 (s, 1H), 9.81 (s, 1H), 8.73 (s, 1H), 8.07 (s, 1H), 7.58 (t, J = 6.8 Hz, 1H), 7.39 (s, 1H),

7.27 (dd, J = 13.2, 8.0 Hz, 1H), 6.75 (s, 1H), 6.69 (s, 1H), 2.32 (s, 3H). LRMS (ESI) calcd for $C_{18}H_{14}FN_5O_2$ $[M+H]^+$: 352.35, found 352.33.

4-amino-6-fluoro-8-(6-methyl-2-oxo-2,3-dihydro-1H-benzo[d]imidazol-5-yl)quinoline-3-carboxamide (24). White solid. Yield: 50%. ^{1}H NMR (400MHz, DMSO-d_6, ppm) δ 10.54 (s, 1H), 9.91 (s, 1H), 8.73 (s, 1H), 8.49 (s, 2H), 8.16 (d, J = 10.5 Hz, 1H), 8.03 (s, 1H), 7.53 (d, J = 7.8 Hz, 1H), 7.34 (s, 1H), 6.77 (s, 2H), 2.33 (s, 3H). LRMS (ESI) calcd for $C_{18}H_{14}FN_5O_2$ $[M+H]^+$: 352.35, found 352.43.

4-amino-5-fluoro-8-(5-methoxy-1H-indazol-6-yl)quinoline-3-carboxamide (25). White solid. Yield: 60%. ^{1}H NMR (400MHz, DMSO-d_6, ppm) δ 12.87 (s, 1H), 8.65 (s, 1H), 7.99 (s, 2H), 7.55 (dd, J = 8.0, 6.2 Hz, 1H), 7.36 (s, 1H), 7.25-7.24 (m, 3H), 3.61 (s, 3H). ^{13}C NMR (100MHz, DMSO-d_6, ppm) δ 170.5, 159.4 (d, J = 252 Hz), 152.5, 152.4, 150.1, 149.0, 135.2, 134.6 (d, J = 3 Hz), 132.8, 131.7 (d, J = 10 Hz), 125.3, 122.5, 112.4, 109.3 (d, J = 23 Hz), 108.4 (d, J = 7 Hz), 103.2, 99.1, 55.6. ^{19}F NMR (376MHz, DMSO-d_6, ppm) δ -113.0. LRMS (ESI) calcd for $C_{18}H_{14}FN_5O_2$ $[M+H]^+$: 352.35, found 352.42. HPLC purity: 98%. t_R = 11.55 min.

General procedure for the synthesis of intermediates 30a-d.

Step 1. A solution of aniline **26a-d** (10 mmol) and ethyl ethoxymethylenemalonate (4 mL, 10 mmol) was heated at 100 °C for 2 h. Then the molten mass was added slowly onto the boiling Dowtherm A (10 mL) and the mixture was heated at reflux for 4-12 h. After the mixture cooled to rt, the precipitated solid was collected by filtration and dried to afford the product.

Step 2. Ethyl quinoline-3-carboxylate **27a-d** (6.4 mmol) were dissolved in THF:EtOH:H_2O (4:4:2, 50 mL) and added lithium hydroxide (3 equiv.). The resulting mixture was heated at 55 °C for 4-8 h, after which the volatile solvent was evaporated to give an aqueous phase which was acidified to pH=3 with 1.5 N HCl aqueous solution. The resulting precipitate was filtered and dried to yield quinoline-3-carboxylic acid **28a-d**, which was used without further purification. A solution of quinoline-3-carboxylic acid **28a-d** (3.5 mmol) in $SOCl_2$ (5 mL) and cat. DMF (two drops) was heated to 70 °C for 3-6 h. The reaction mixture was then concentrated under reduced pressure to obtain a

residue which was then dissolved in DCM (50 mL) and 25% aq. ammonia (50 mL) was added at 0 °C. The resulting precipitate was filtered to obtain the desired amide **29a-d**.

Step3. The amide **29a-d** was placed in the sealed tube and dissolved in 7M ammonium methanol solution. The reaction mixture was heated at 80 °C overnight. The precipitated solid was collected by filtration and dried to afford the product **30a-d**.

4-amino-8-bromoquinoline-3-carboxamide (30a). White solid. Total yield: 10%. ^{1}H NMR (400MHz, DMSO-d_6, ppm) δ 8.89 (s, 1H), 8.60 (s, 1H), 8.33 (d, J = 8.4 Hz, 1H), 8.07-8.05 (m, 2H), 7.40 (s, 1H), 7.37 (t, J = 8.0 Hz, 1H).

4-amino-8-bromo-5-fluoroquinoline-3-carboxamide (30b). White solid. Total yield: 16%. ^{1}H NMR (400MHz, DMSO-d_6, ppm) δ 8.88 (s, 1H), 8.15 (s, 1H), 8.06 (dd, J = 8.4, 5.2 Hz, 1H), 7.51 (s, 1H), 7.22 (d, J = 13.2, 8.4 Hz, 1H).

4-amino-8-bromo-6-fluoroquinoline-3-carboxamide (30c). White solid. Total yield: 14%. ^{1}H NMR (400MHz, DMSO-d_6, ppm) δ 8.87 (s, 1H), 8.56 (s, 1H), 8.24 (m, 1H), 8.10 (dd, J = 7.8, 2.4 Hz, 1H), 7.45 (s, 1H).

4-amino-8-bromo-6-nitroquinoline-3-carboxamide (30d). White solid. Total yield: 6%. ^{1}H NMR (400MHz, DMSO-d_6, ppm) δ 9.21 (s, 1H), 9.07 (d, J = 2.3 Hz, 1H), 8.93 (d, J = 2.3 Hz, 1H), 8.33 (s, 1H), 8.17 (s, 1H).

4-bromo-2,6-difluorobenzaldehyde (32). In a round-bottom flask, *n*-butyl lithium (8.8 mL, 22 mmol) was added dropwise to a solution of diisopropyl amine (3.2 mL, 22 mmol) in dry THF at -78°C under nitrogen atmosphere over a period of 5 minutes. Then the mixture was warmed to -20°C and stirred for another 25 minutes. 1-bromo-3,5-difluorobenzene **31** (2.4 mL, 20 mmol) in dry THF (10 mL) was added at -78°C, continued stirring for a further 25 minutes, followed by the addition of DMF (1.7 mL, 22 mmol) in dry THF at -78°C. The resulting mixture was stirred at room temperature for 2 h. The reaction was quenched by ammonium chloride solution. Then the organic solvent was removed under the reduced pressure. The residue was dissolved in DCM, and extracted by water for three times. Purification by column chromatography on silica gel (2% ethyl acetate in hexane) afforded 2.3 g of the product (50% yield). ^{1}H NMR (400MHz, $CDCl_3$, ppm) δ 10.29 (s, 1H), 7.26-7.21 (m, 2H).

General procedure for the synthesis of intermediates 35a-h.

Step 1. To a suspension of **32** (1.1 g, 5 mmol) and K_2CO_3 (1.0 g, 7.5 mmol) in *N,N*-dimethylacetamide (5 mL) was added corresponding substituted phenol or aniline (1 equiv.) . The resulting mixture was stirred at 100 ^oC for 4 h. After cooling to rt, the suspension was extracted with EtOAc and water. The organic layer was collected and concentrated under vacuum. Purification by column chromatography on silica gel (1% ethyl acetate in hexane) afforded corresponding products **33b-h** (35-61% yield).

Step 2. Hydrazinehydrate (10 mL) was added over 5 min to a solution of the prepared aldehyde **33b-h** or readily available 4-bromo-2-fluorobenzaldehyde **33a** (10 mmol) in DME (10 mL). The reaction mixture was refluxed for 15 h and concentrated in vacuo to approximately 10 mL. Water (10-20 mL) was added to the mixture. The resulting product precipitate was filtered off and dried in vacuo to provide the 1*H*-indazole **34a-h** as solid.

Step 3. A solution of **34a-h** (200 mg, 1.02 mmol) in anhydrous THF (4 mL) was treated dropwise with *tert*-butyllithium (1.3 M solution in pentane, 2.6 mL, 3.4 mmol). After

stirring for 25 minutes the mixture was treated dropwise with tributyl borate (0.83 mL, 3.06 mmol) and allowed to warm up to room temperature. After stirring overnight the reaction mixture was quenched by saturated ammonium chloride solution and concentrated under vacuum. The resulting residue was dissolved in sodium hydroxide solution (20 mL, 1M) and washed by DCM. Then the aqueous layer was acidified with conc. HCl solution to pH=2, extracted with ether. The combined ether extracts were dried over sodium sulfate and concentrated to obtain (1*H*-indazol-6-yl)boronic acid **35a-h** as a solid, which was used for the next step without further purification.

5-bromo-2,4-dimethylaniline (37a). To a suspension of 1-bromo-2,4-dimethyl-5-nitrobenzene **36a** (9.2 g, 40 mmol) and NH_4Cl (1.5 g, 28 mmol) in ethanol (25 mL) and water (10 mL) was added iron powder (13.4 g, 240 mmol). The reaction mixture was heated at 80 ^oC for 1 h. The iron was removed by filtration and the filtrated was concentrated to dryness. The resulting residue was dissolved in DCM and washed by brine for three times. The organic phase was dried over sodium sulfate and

concentrated to obtain 5-bromo-2,4-dimethylaniline **37a** (6.4 g, 80% yield) as a yellow solid, which was used for the next step without further purification.

5-bromo-4-methoxy-2-methylaniline (37b). To a suspension of 1-bromo-2-methoxy-4-methyl-5-nitrobenzene **36b** (9.9 g, 40 mmol) and NH_4Cl (1.5 g, 28 mmol) in ethanol (25 mL) and water (10 mL) was added iron powder (13.4 g, 240 mmol). The reaction mixture was heated at 80 ^oC for 1 h. The iron was removed by filtration and the filtrated was concentrated to dryness. The resulting residue was dissolved in DCM and washed by brine for three times. The organic phase was dried over sodium sulfate and concentrated to obtain 5-bromo-4-methoxy-2-methylaniline **37b** (7.8 g, 90% yield) as a yellow solid, which was used for the next step without further purification.

tert-butyl 6-bromo-5-methyl-1H-indazole-1-carboxylate (38a).

Step 1: Aniline **37a** (4.0 g, 20 mmol) was added to a 50% aqueous solution of fluroboric acid (20 mL) at rt and stirred for 5 min. The mixture was cooled to 0 ^oC and an aqueous solution of $NaNO_2$ (1.7 g, 24 mmol) was added. The reaction mixture was stirred at 10 ^oC for 3 h, during which the product precipitated. The cooled suspension

was filtrated and the solid product washed with small amount of water, methanol and ether. The resulting solid was dried under high vacuum.

Step 2. The solution of 18-crown-6 (185 mg, 0.7 mmol) and potassium acetate (2.7 g, 28 mmol) in dry $CHCl_3$ was stirred at rt for 10 min. Then the solid resulted from step 1 (4.2 g, 14 mmol) was added to the solution in small portions under N_2 atmosphere. The reaction mixture was stirred at rt for 3 h. The suspension was filtrated and the residue was washed with $CHCl_3$. The organic layer was washed with water and concentrated in vacuo to give the crude product.

Step 3. The product from step 2 (2.1 g, 10 mmol) and DMAP (244 mg, 2 mmol) were dissolved in acetonitrile (20 mL). Et_3N (2.4 ml, 17 mmol) and di-*tert*-butyl carbonate (3.0 mL, 13 mmol) were added to the solution. Then the reaction mixture was stirred at rt for 1 h. The brown solution was evaporated to dryness. The residue was dissolved in DCM and washed with brine. The organic phase was collected and concentrated under the vacuum. Purification by column chromatography on silica gel (eluting with petroleum ether-ethyl acetate, 4:1) afforded the desired compound **38a** (2.2 g, 35% yield).

tert-butyl 6-bromo-5-methoxy-1H-indazole-1-carboxylate (38b). The synthesis of **38b** was the same as described as **38a**. Purification by column chromatography on silica gel (eluting with petroleum ether-ethyl acetate, 4:1) afforded the desired compound **38b** (1.6 g, 25% yield).

5-methyl-6-(4,4,5,5-tetramethyl-1,3,2-dioxaborolan-2-yl)-1H-indazole (39a). *tert*-butyl 6-bromo-5-methyl-1*H*-indazole-1-carboxylate **38a** (1.6 g, 5 mmol) is dissolved in argon purged anhydrous 1,4-dioxane (10 mL). To this solution is added bis(pinacolato)diboron (1.5 g, 6 mmol), KOAc (0.98 g, 10 mmol), and Pd(dppf)Cl_2 (0.36 g, 0.5 mmol). The reaction is heated to 95 °C overnight under argon atmosphere then cooled to rt and diluted with brine and EtOAc. The organic layer was evaporated to dryness then purified by column chromatography on silica gel (eluting with petroleum ether-ethyl acetate, 4:1). The resulting product in DCM (2 mL) was treated with TFA (2 mL). The reaction mixture was stirred at rt for 1 h then concentrated to obtain **39a** (0.77 g, 60% yield) as a dark solid, which could be used for the next step without further purification. ^{1}H NMR

(400MHz, $CDCl_3$, ppm) δ 10.84 (s, 1H), 8.01 (s, 2H), 7.52 (s, 1H), 2.64 (s, 3H), 1.39 (s, 12H).

5-methoxy-6-(4,4,5,5-tetramethyl-1,3,2-dioxaborolan-2-yl)-1H-indazole (39b). *tert*-butyl 6-bromo-5-methyl-1*H*-indazole-1-carboxylate **38b** (1.5 g, 4.6 mmol) is dissolved in argon purged anhydrous 1,4-dioxane (10 mL). To this solution is added bis(pinacolato)diboron (1.4 g, 5.5 mmol), KOAc (0.9 g, 9.2 mmol), and $Pd(dppf)Cl_2$ (0.34 g, 0.46 mmol). The reaction is heated to 95 °C overnight under argon atmosphere then cooled to rt and diluted with brine and EtOAc. The organic layer was evaporated to dryness then purified by column chromatography on silica gel (eluting with petroleum ether-ethyl acetate, 4:1). The resulting product in DCM (2 mL) was treated with TFA (2 mL). The reaction mixture was stirred at rt for 1 h then concentrated to obtain **39b** (0.7 g, 55% yield) as a dark solid, which could be used for the next step without further purification. ^{1}H NMR (400MHz, $CDCl_3$, ppm) δ 7.96 (s, 1H), 7.83 (s, 1H), 7.06 (s, 1H), 3.84 (s, 3H), 1.37 (s, 12H).

General procedure for the synthesis of intermediate 42.

Step1. A solution of 1,2-diaminobenzene **40** (10 mmol) in DMF (10 mL) was treated with *N, N'*-carbonyldiimidazole (2 equiv.) and stirred at room temperature for 18 h. After removal of the DMF in vacuo, the resulting white solid was washed with H_2O and dried on high vacuum to give **41** (75-78%) as a white solid.

Step 2. 5-Bromo-1,3-dihydro-benzoimidazol-2-one **41** (5 mmol) is dissolved in argon purged anhydrous DMF (5 mL). To this solution is added bis(pinacolato)diboron (1.2 equiv.), KOAc (3 equiv.), and $PdCl_2$(dppf), 1:1 complex with CH_2Cl_2 (0.1 equiv.). The reaction is heated to 95 °C overnight with mechanical stirring then cooled to room temperature and diluted with brine (50 mL) and EtOAc (75 mL). The mixture is filtered to remove a dark brown solid, which is washed thoroughly with EtOAc. The layers are separated and the organics washed with water, then dried with anhydrous $MgSO_4$, filtered and evaporated under reduced pressure. Trituration with 1:1 CH_2Cl_2/hexanes affords the products **42** (80-83%)

Cell culture: Ramos cells was cultured complete growth medium RPMI 1640 supplemented with 10% FBS and 1% Penicillin-Streptomycin and grown at 37 °C with 5% CO_2.

Antibodies: Anti-BTK antibody was purchased from Absin (abs135992, 1:1,000 dilution). Anti-BTK (phospho Y223) antibody was purchased from Abcam (ab68217, 1:1,000 dilution). Anti-GAPDH antibodies was purchased from CWBIO (CW0100M, 1:2,000 dilution). Anti-mouse IgG-HRP, and anti-rabbit IgG-HRP were purchased from Cell Signaling Technology and used at 1:5,000 dilution.

BTK enzymatic assay: BTK enzymatic activity was determined with the off-chip mobility shift assay. The compound was diluted to 50x of the final concentration with DMSO. Add 10 μL of compound into 90 μL of 1x kinase buffer (50 mM HEPES, pH 7.5, 0.01% Brij-35) and mix the solution for 10 min on shaker. Transfer 5 μL of the diluted solution into a 384-well plate in triplicates. 10 uL of 1x kinase base buffer containing BTK^{WT} (Carna, Cat. No 08-180) or BTK^{C481S} (Carna, Cat. No 08-547) was added into the 384-well plate, and incubated with compound for 10 min. Then 10 uL of 1x kinase

buffer containing FAM-labeled peptide (GL Biochem, Cat. No. 112394, Lot. No. P131014-XP112394) and ATP (Sigma, Cat. No. A7699-1G, CAS No. 987-65-5) was added. Incubated at 28 ^{o}C for specified period of time. Adding 25 µL of stop buffer (100 mM HEPES, pH 7.5, 0.015% Brij-35, 0.2% Coating Reagent #3, 50 mM EDTA) to stop reaction. Collect data on Caliper.

Percent inhibition = (max-conversion)/(max-min)*100.

"max" stands for DMSO control; "min" stands for low control.

Fit the data in XLfit excel add-in version 4.3.1 obtain IC_{50} values.

Equation used is

Y=Bottom + (Top-Bottom)/(1+(LogIC_{50}/X)*HillSlope)

The results represented as mean ± SD from at least three separate assays performed in triplicates.

EGFR inhibition assay: EGFR assay was detected by Z'-LYTETM kinase assay kit (Invitrogen, PV3193). The test compounds were diluted to 3-fold serial dilutions in aqueous solution (containing 4% DMSO). The fluorescence signals were detected at

400 nm (excitation) and 445/520 nm (emission) using an EnVision multilabel plate reader (PerkinElmer Life Sciences, Boston, MA, USA). The IC_{50} values represented as mean from at least three separate assays performed in triplicates.

TEC inhibition assay: Tec kinase (Carna, Cat. No 08-182) enzymology assays were performed according to the protocols specified in HTRF® KinEase™ assays sold by Cisbio Bioassays. Basically, kinase and substrate were mixed with various concentrations of compounds at rt, followed by addition of ATP to start enzymatic reactions. After 1 h, the reactions were stopped by EDTA detection solution, and then europilated antiphosphotyrosine antibodies and streptavidin XL665 conjugates were added. The mixtures were incubated at rt for another 1 h and read by EnVision multilabel plate reader. Data analysis was performed with GraphPad Prism 7. The results represented as mean from at least three separate assays performed in triplicates.

YES inhibition assay: YES (Eurofins, Cat. No 14-178) is incubated with 8 mM MOPS pH 7.0, 0.2 mM EDTA, 0.1 mg/mL poly(Glu, Tyr) 4:1, 10 mM magnesium acetate and

[gamma-^{33}P]-ATP (specific activity and concentration as required). The reaction is initiated by the addition of the Mg/ATP mixture at room temperature. After incubation for 40 minutes, the reaction is stopped by the addition of phosphoric acid to a final concentration of 0.5%. 10 uL of the reaction mixture is then spotted onto a Filtermat A and washed four times by 0.425% phosphoric acid and once by methanol before drying and scintillation counting. The results represented as mean from at least three separate assays performed in triplicates.

ITK inhibition assay: ITK (Eurofins, Cat. 14-660) is incubated with 8 mM MOPS pH 7.0, 0.2 mM EDTA, 0.33 mg/mL myelin basic protein, 10 mM magnesium acetate and [gamma-^{33}P]-ATP (specific activity and concentration as required). The reaction is initiated by the addition of the Mg/ATP mix. After incubation for 40 minutes at room temperature, the reaction is stopped by the addition of phosphoric acid to a concentration of 0.5%. 10 uL of the reaction is then spotted onto a P30 filtermat and washed four times for 4 minutes in 0.425% phosphoric acid and once in methanol prior

to drying and scintillation counting. The results represented as mean from at least three separate assays performed in triplicates.

SRC inhibition assay: SRC (Eurofins, Cat. 23-042) is incubated with 8 mM MOPS pH 7.0, 0.2 mM EDTA, 250 uM KVEKIGEGTYGVVYK (Cdc2 peptide), 10 mM magnesium acetate and [gamma-^{33}P]-ATP (specific activity and concentration as required). The reaction is initiated by the addition of the Mg/ATP mixture at room temperature. After incubation for 40 minutes, the reaction is stopped by the addition of phosphoric acid to a final concentration of 0.5%. 10 uL of the reaction mixture is then spotted onto a Filtermat A and washed four times by 0.425% phosphoric acid and once by methanol before drying and scintillation counting. The results represented as mean from at least three separate assays performed in triplicates.

FYN inhibition assay: FYN (Eurofins, Cat. 14-441) is incubated with 50 mM Tris pH 7.5, 0.1 mM EGTA, 0.1 mM Na_3VO_4, 250 uM KVEKIGEGTYGVVYK (Cdc2 peptide), 10 mM magnesium acetate and [gamma-^{33}P]-ATP (specific activity and concentration as required). The reaction is initiated by the addition of the Mg/ATP mix. After incubation

for 40 minutes at room temperature, the reaction is stopped by the addition of phosphoric acid to a concentration of 0.5%. 10 uL of the reaction is then spotted onto a P30 filtermat and washed four times for 4 minutes in 0.425% phosphoric acid and once in methanol prior to drying and scintillation counting. The results represented as mean from at least three separate assays performed in triplicates.

BLK inhibition assay: BLK (Eurofins, Cat. 14-316) is incubated with 50 mM Tris pH 7.5, 0.1 mM EGTA, 0.1 mM Na_3VO_4, 0.1% 6-mercaptoethanol, 0.1 mg/mL poly(Glu, Tyr) 4:1, 10 mM magnesium acetate and [gamma-^{33}P]-ATP (specific activity and concentration as required). The reaction is initiated by the addition of the Mg/ATP mixture at room temperature. After incubation for 40 minutes, the reaction is stopped by the addition of phosphoric acid to a final concentration of 0.5%. 10 uL of the reaction mixture is then spotted onto a Filtermat A and washed four times by 0.425% phosphoric acid and once by methanol before drying and scintillation counting. The results represented as mean from at least three separate assays performed in triplicates.

Cellular BTK phosphorylation: Ramos cells were plated in 12 well volume plate at 1.6 x 10^6 cells per well, compounds diluted in RPMI 1640 media were added to the cells. After 2 hours incubation, the cells were treated with activator solution (1.9 mM H_2O_2 and 5 mM Na_3VO_4) for 15 min. Cells were lysed with RIPA lysis buffer, the phosphorylation levels of BTK (Tyr223) were analyzed by western blotting. The results represented as mean ± SD from at least three separate assays performed in triplicates.

***In vitro* plasma stability:** Compound with initial concentration of 1 μM was incubated in human, beagle dog, SD rat, mouse and monkey plasma samples for 2 h at 37 ^oC. Then the samples were quenched by adding 10 volumes of 100% methanol supplemented with internal standard and centrifuged at 12,000 rpm for 5 min. Following that, the supernatants were transferred to a new plate containing an equal volume of water for analysis by liquid chromatography coupled to triple quadrupole mass spectrometry (LC–MS/MS). The results represented as mean from three separate assays performed in triplicates.

Animals. All animal care and experimental protocols were performed in accordance with the "Guide for the Care and Use of Laboratory Animals"(National Institutes of Health Publication, revised 1996, No. 86-23, Bethesda, MD) and approved by the Institutional Animal Care and Use Committee (IACUC) of Tsinghua University. Male Sprague-dawley rats with a body weight of 187-205 g at 5−7 weeks old and male DBA/1 mice of 18-20 g at 4−6 weeks old were purchased from Shanghai Slac Laboratory Animal Ltd., Shanghai, China.

***In Vivo* Pharmacokinetics Study:** A single dose of compound **25** (2 mg/kg in 10% DMSO and 90% PEG400) was administered by tail vein injection to fed male Sprague-dawley rats (n=6). Compound **25** was also dosed orally (5 mg kg^{-1}) as a suspension in 0.5% methylcellulose to fasted male Sprague-dawley rats (n=6). Blood samples (~0.2 mL) were obtained via a jugular cannula at pre-dose, 0.033 (IV only), 0.25, 0.5, 1, 2, 4, 6, 8, 10 and 24 hr post dose. Blood was centrifuged at 4000rpm for 15 min at 4 ^{o}C, and plasma was collected and stored at -20 °C until analysis by LC-MS/MS. Serial PK profiles were generated for each dosing group.

Mice collagen induced arthritis (CIA) study: Male DBA/1 mice were immunized intradermally at the base of the tail with bovine collagen type II emulsified in Complete Freund's Adjuvant (CFA) on day 0; on day 20, mice were challenged with collagen type II in Incomplete Freund's Adjuvant (IFA). On day 29, the CIA model mice were randomized and treated orally with 0.2 mg/kg dexamethasone (n=6), 10 mg/kg compound **25** (n=6) and vehicle control (n=6) QD. Paw thickness measurements by a caliper were performed throughout the day.

Docking simulations of BTK inhibitors: Prediction of ligand binding to BTK was done with Schrodinger Suite 2017-1. Processing of the protein structure was performed with the Protein Preparation Wizard. Converting of ligands from 2D to 3D structures was performed using LigPrep. Molecular docking was performed with Glide.

Solubility determinations: The dry powder was equilibrated with 0.1 M phosphate buffer (pH 7.4) in a glass vial at 25 °C (water bath), shaking for 24 h. After filtration using a 0.45 μm PVDF membrane filter, the concentration of corresponding compound was determined by HPLC, comparing the peak area obtained with that from a standard

solution of the compound in DMSO. The results represented as mean from three separate assays performed in triplicates.

ASSOCIATED CONTENT

Supporting Information.

The Supporting Information is available free of charge on the ACS Publications website at DOI:

Western blotting data for evaluation EC_{50} values of compounds **6** and **25**, analytical RP-HPLC trace(s) for compound **6**, **7**, **17** and **25** and NMR spectra of all new compounds (PDF)

Docking model of compound **7** (PDB)

Docking model of compound **25** (PDB)

Molecular formula strings (CSV)

AUTHOR INFORMATION

Corresponding Author

*yrao@tsinghua.edu.cn;

Author Contributions

The manuscript was written through contributions of all authors. All authors have given approval to the final version of the manuscript. ‡These authors contributed equally.

Funding Sources

This work was supported by the National Natural Science Foundation of China (#81573277, 81622042, 81773567), National Major Scientific and Technological Special Project for “Significant New Drugs Development” (#SQ2017ZX095003, 2018ZX09711001) and Tsinghua University Initiative Scientific Research Program. This work was also financially supported by the NSFC (No. 81670187) and Beijing Natural Science Foundation (No. 7172047).

Notes

The authors declare no competing financial interest.

ACKNOWLEDGMENT

We would like to thank Prof. Qinghua, Tao for providing cell culture room. This work was supported by the National Natural Science Foundation of China (#81573277, 81622042, 81773567), National Major Scientific and Technological Special Project for "Significant New Drugs Development" (#SQ2017ZX095003, 2018ZX09711001) and Tsinghua University Initiative Scientific Research Program. This work was also financially supported by the NSFC (No. 81670187) and Beijing Natural Science Foundation (No. 7172047).

ABBREVIATIONS

BTK, bruton's tyrosine kinase; RA, rheumatoid arthritis; CIA, collagen-induced arthritis; NSAIDs, non-steroidal anti-inflammatory drugs; DMARDs, disease-modifying anti-rheumatic drugs; MTX, methotrexate; SLE, systemic lupus erythematosus; BCR, B cell receptor; MCL, mantle-cell lymphoma; CLL, chronic lymphocytic leukemia; WM, Waldenström's macroglobulinemia; Aq. Sol., aqueous solubility; PK, pharmacokinetic; EGFR, epidermal growth factor receptor; DXMS, dexamethasone; LDA, lithium diisopropylamide; DMF, *N,N*-dimethylformamide; THF, tetrahydrofuran; DMA, *N,N*-

dimethylacetamide; DME, 1,2-dimethoxyethane; RT, room temperature; DMAP, 4-dimethylaminopyridine; TFA, trifluoroacetic acid; DCM, dichloromethane; TLC, thin layer chromatography.

REFERENCES

1. Mcinnes, I. B.; Schett, G. The pathogenesis of rheumatoid arthritis. *N. Engl. J. Med.* **2011**, *365*, 2205-2219.

2. Smolen, J.S.; Aletaha, D. Rheumatoid arthritis therapy reappraisal: strategies, opportunities and challenges. *Nat. Rev. Rheumatol.* **2015**, *11*, 256-289.

3. Kremer, J.M.; Bloom, B.J.; Breedveld, F.C.; Coombs, J.H.; Fletcher, M.P.; Gruben, D.; Krishnaswami, S.; Burgos-Vargas,R.; Wilkinson, B.; Zerbini, C.A.F.; Zwillich, S.H. The safety and efficacy of a JAK inhibitor in patients with active rheumatoid arthritis: Results of a double-blind, placebo-controlled phase IIa trial of three dosage levels of CP-690,550 versus placebo. *Arthritis Rheum.* **2009**, *60*, 1895-1905.

4. Gadina, M. Advances in kinase inhibition: treating rheumatic diseases and beyond. *Curr. Opin. Rheumatol.* **2014**, *26*, 237-243.

5. Whyburn, L. R.; Halcomb, K. E.; Contreras, C. M.; Lowell, C. A.; Witte, O. N.; Satterthwaite, A. B. Reduced dosage of Bruton's tyrosine kinase uncouples B cell hyperresponsiveness from autoimmunity in lyn-/- mice. *J. Immunol.* **2003**, *171*, 1850-1858.

6. Brunner, C.; Müller, B.; Wirth, T. Bruton's tyrosine kinase is involved in innate and adaptive immunity. *Histol. Histopathol.* **2005**, *20*, 945-955.

7. Satterthwaite, A. B.; Li, Z.; Witte, O. N. Btk function in B cell development and response. *Semin. Immunol.* **1998**, *10*, 259-316.

8. Khan, W. N. Regulation of B lymphocyte development and activation by Bruton's tyrosine kinase. *Immunol. Res.* **2001**, *23*, 147-156.

9. Kil, L.P.; de Bruijn, M.J.; Van, N.M.; Corneth,O.B.; van Hamburg, J.P.; Dingjan, G.M.; Thaiss, F.; Rimmelzwaan, G.F.; Elewaut, D.; Delsing, D. Btk levels set the threshold for B-cell activation and negative selection of autoreactive B cells in mice. *Blood* **2012**, *119*, 3744-3756.

10. Whang, J. A.; Chang, B. Y. Bruton's tyrosine kinase inhibitors for the treatment of rheumatoid arthritis. *Drug Discov. Today* **2014**, *19*, 1200-1204.

11. Norman, P. Investigational Bruton's tyrosine kinase inhibitors for the treatment of rheumatoid arthritis. *Expert Opin. Investig. Drugs* **2016**, *25*, 891-899.

12. Lou, Y.; Owens, T. D.; Kuglstatter, A.; Kondru, R. K.; Goldstein, D. M. Bruton's tyrosine kinase inhibitors: Approaches to potent and selective inhibition, preclinical and clinical evaluation for inflammatory diseases and B cell malignancies. *J. Med. Chem.* **2012**, *55*, 4539-4550.

13. Hendriks, R. W.; Yuvaraj, S.; Kil, L. P. Targeting Bruton's tyrosine kinase in B cell malignancies. *Nat. Rev. Cancer* **2014**, *14*, 219-232.

14. Liang, C.; Tian, D.; Ren, X.; Ding, S.; Jia, M.; Xin, M.; Thareja, S. The development of Bruton's tyrosine kinase (BTK) inhibitors from 2012 to 2017: A mini-review. *Eur. J. Med. Chem.* **2018**, *151*, 315-326.

15. Xue, Y.; Song, P.; Song, Z.; Wang, A.; Tong, L.; Geng, M.; Ding, J.; Liu, Q.; Sun, L.; Xie, H.; Zhang, A. Discovery of 4,7-Diamino-5-(4-phenoxyphenyl)-6-methylene-

pyrimido[5,4-*b*]pyrrolizines as Novel Bruton's Tyrosine Kinase Inhibitors. *J. Med. Chem.* **2018**, *61*, 4608-4625.

16. Pan, Z.; Scheerens, H.; Li, S.; Schultz, B. E.; Sprengeler, P. A.; Burrill, L. C.; Mendonca, R. V.; Sweeney, M. D.; Scott, K. C. K.; Grothaus, P. G.; Jeffery, D. A.; Spoerke, J. M.; Honigberg, L. A.; Young, P. R.; Dalrymple, S. A.; Palmer, J. T. Discovery of selective irreversible inhibitors for Bruton's tyrosine kinase. *ChemMedChem* **2007**, *2*, 58-61.

17. Honigberg, L. A.; Smith, A. M.; Sirisawad, M.; Verner, E.; Loury, D.; Chang, B.; Li, S.; Pan, Z.; Thamm, D. H.; Miller, R. A.; Buggy, J. J. The Bruton tyrosine kinase inhibitor PCI-32565 blocks B-cell activation and is efficacious in models of autoimmune disease and B-cell malignancy. *Proc. Natl. Acad. Sci. USA* **2010**, *107*, 12575-12580.

18. Advani, R. H.; Buggy, J. J.; Sharman, J. P.; Smith, S. M.; Boyd, T. E.; Grant, B.; Kolibaba, K. S.; Furman, R. R.; Rodriguez, S.; Chang, B. Y.; Sukbuntherng, J.; Izumi, R.; Hamdy, A.; Hedrick, E.; Fowler, N. H. Bruton tyrosine kinase inhibitor ibrutinib (PCI-

32565) has significant activity in patients with relapsed/refractory B-cell malignancies. *J. Clin. Oncol.* **2013**, *31*, 88-94.

19. Byrd, J. C.; Furman, R. R.; Coutre, S. E.; Flinn, I. W.; Burger, J. A.; Blum, K. A.; Grant, B.; Sharman, J. P.; Coleman, M.; Wierda, W. G.; Jones, J. A.; Zhao, W.; Heerema, N. A.; Johnson, A. J.; Sukbuntherng, J.; Chang, B. Y.; Clow, F.; Hedrick, E.; Buggy, J. J.; James, D. F.; O'Brien, S. Targeting BTK with ibrutinib in relapsed chronic lymphocytic leukemia. *N. Engl. J. Med.* **2013**, *369*, 32-42.

20. Wang, M. L.; Rule, S.; Martin, P.; Goy, A.; Auer, R.; Kahl, B. S.; Jurczak, W.; Advani, R. H.; Romaguera, J. E.; Williams, M. E. Targeting BTK with ibrutinib in relapsed or refractory mantle-cell lymphoma. *N. Engl. J. Med.* **2013**, *369*, 507-516.

21. Treon, S. P.; Tripsas, C. K.; Meid, K.; Warren, D.; Varma, G.; Green, R.; Argyropoulos, K. V.; Yang, G.; Cao, Y.; Xu, L.; Patterson, C. J.; Rodig, S.; Zehnder, J. L.; Aster, J. C.; Harris, N. L.; Kanan, S.; Ghobrial, I.; Castillo, J. J.; Laubach, J. P.; Hunter, Z. R.; Salman, Z.; Li, J.; Cheng, M.; Clow, F.; Graef, T.; Palomba, M. L.; Advani,

R. H. Ibrutinib in previously treated Waldenstrom's macroglobulinemia. *N. Engl. J. Med.* **2015**, *372*, 1425-1440.

22. Noy, A.; Vos, S. D.; Thieblemont, C.; Martin, P.; Flowers, C. R.; Morschhauser, F.; Collins, G. P.; Ma, S.; Coleman, M.; Peles, S. Targeting Bruton tyrosine kinase with ibrutinib in relapsed/refractory marginal zone lymphoma. *Blood* **2017**, *129*, 2224-2232.

23. Evans, E. K.; Tester, R.; Aslanian, S.; Karp, R.; Sheets, M.; Labenski, M. T.; Witowski, S. R.; Lounsbury, H.; Chaturvedi, P.; Mazdiyasni, H.; Zhu, Z.; Nacht, M.; Freed, M. I.; Petter, R. C.; Dubrovskiy, A.; Singh, J.; Westlin, W. F. Inhibition of Btk with CC-292 provides early pharmacodynamic assessment of activity in mice and humans. *J. Pharmacol. Exp. Ther.* **2013**, *346*, 219-228.

24. Wu, J.; Zhang, M.; Liu, D. Acalabrutinib (ACP-196): a selective second-generation BTK inhibitor. *J. Hematol. Oncol.* **2016**, 9, 9:21.

25. Herman, S. E. M.; Montraveta, A.; Niemann, C. U.; Mora-Jensen, H.; Gulrajani, M.; Krantz, F.; Mantel, R.; Smith, L. L.; McClanahan, F.; Harrington, B. K.; Colomer, D.; Covey, T.; Byrd, J. C.; Izumi, R.; Kaptein, A.; Ulrich, R.; Johnson, A. J.; Lannutti, B. J.;

Wiestner, A.; Woyach, J. A. The Bruton tyrosine kinase (BTK) inhibitor Acalabrutinib demonstrates potent on-target effects and efficacy in two mouse models of chronic lymphocytic leukemia. *Clin. Cancer Res.* **2017**, *23*, 2831-2841.

26. Liu, Q.; Sabnis, Y.; Zhao, Z.; Zhang, T.; Buhrlage, S. J.; Jones, L. H.; Gray, N. S. Developing irreversible inhibitors of the protein kinase cysteinome, *Chem. Biol.* **2013**, *20*, 146-159.

27. Liu, L.; Di Paolo, J.; Barbosa, J.; Rong, H.; Reif, K.; Wong, H. Antiarthritis effect of a novel Bruton's tyrosine kinase (BTK) inhibitor in rat collagen-induced arthritis and mechanism-based pharmacokinetic/pharmacodynamic modeling: relationships between inhibition of BTK phosphorylation and efficacy. *J. Pharmacol. Exp. Ther.* **2011**, *338*, 154-163.

28. Di Paolo, J. A.; Huang, T.; Balazs, M.; Barbosa, J.; Barck, K. H.; Bravo, B. J.; Carano, R. A. D.; Darrow, J.; Davies, D. R.; DeForge, L. E.; Diehl, L.; Ferrando, R.; Gallion, S. L.; Giannetti, A. M.; Gribling, P.; Hurez, V.; Hymowitz, S. G.; Jones, R.; Kropf, J. E.; Lee, W. P.; Maciejewski, P. M.; Mitchell, S. A.; Rong, H.; Staker, B. L.;

Whitney, J. A.; Yeh, S.; Young, W. B.; Yu, C.; Zhang, J.; Reif, K.; Currie, K. S. Specific Btk inhibition suppresses B cell- and myeloid cell-mediated arthritis. *Nat. Chem. Biol.* **2011**, *7*, 41-50.

29. Xu, D.; Kim, Y.; Postelnek, J.; Vu, M. D.; Hu, D.; Liao, C.; Bradshaw, M.; Hsu, J.; Zhang, J.; Pashine, A.; Srinivasan, D.; Woods, J.; Levin, A.; O'Mahony, A.; Owens, T. D.; Lou, Y.; Hill, R. J.; Narula, S.; DeMartino, J.; Fine, J. S. RN486, a selective Bruton's tyrosine kinase inhibitor, abrogates immune hypersensitivity responses and arthritis in rodents. *J. Pharmacol. Exp. Ther.* **2012**, *341*, 90-103.

30. Rankin, A. L.; Seth, N.; Keegan, S.; Andreyeva, T.; Cook, T. A.; Edmonds, J.; Mathialagan, N.; Benson, M. J.; Syed, J.; Zhan, Y.; Benoit, S. E.; Miyashiro, J. S.; Wood, N.; Mohan, S.; Peeva, E.; Ramaiah, S. K.; Messing, D.; Homer, B. L.; Dunussi-Joannopoulos, K.; Nickerson-Nutter, C. L.; Schnute, M. E.; Douhan, J. R. Selective inhibition of BTK prevents murine lupus and antibody-mediated glomerulonephritis. *J. Immunol.* **2013**, *191*, 4540-4550.

31. Shi, Q.; Tebben, A.; Dyckman, A. J.; Li, H.; Liu, C.; Lin, J.; Spergel, S.; Burke, J. R.; McIntyre, K. W.; Olini, G. C.; Strnad, J.; Surti, N.; Muckelbauer, J. K.; Chang, C.; An, Y.; Cheng, L.; Ruan, Q.; Leftheris, K.; Carter, P. H.; Tino, J.; De Lucca, G. V. Purine derivatives as potent Bruton's tyrosine kinase (BTK) inhibitors for autoimmune diseases. *Bioorg. Med. Chem. Lett.* **2014**, *24*, 2206-2211.

32. Lou, Y.; Han, X.; Kuglstatter, A.; Kondru, R. K.; Sweeney, Z. K.; Soth, M.; McIntosh, J.; Litman, R.; Suh, J.; Kocer, B.; Davis, D.; Park, J.; Frauchiger, S.; Dewdney, N.; Zecic, H.; Taygerly, J. P.; Sarma, K.; Hong, J.; Hill, R. J.; Gabriel, T.; Goldstein, D. M.; Owens, T. D. Structure-based drug design of RN486, a potent and selective Bruton's tyrosine kinase (BTK) inhibitor, for the treatment of rheumatoid arthritis. *J. Med. Chem.* **2014**, *58*, 512-516.

33. Liu, Q.; Batt, D. G.; Lippy, J. S.; Surti, N.; Tebben, A. J.; Muckelbauer, J. K.; Chen, L.; An, Y.; Chang, C.; Pokross, M.; Yang, Z.; Wang, H.; Burke, J. R.; Carter, P. H.; Tino, J. A. Design and synthesis of carbazole carboxamides as promising inhibitors of

Bruton's tyrosine kinase (BTK) and Janus kinase 2 (JAK2). *Bioorg. Med. Chem. Lett.* **2015**, *25*, 4265-4269.

34. Zhao, X.; Xin, M.; Huang, W.; Ren, Y.; Jin, Q.; Tang, F.; Jiang, H.; Wang, Y.; Yang, J.; Mo, S.; Xiang, H. Design, synthesis and evaluation of novel 5-phenylpyridin-2(1H)-one derivatives as potent reversible Bruton's tyrosine kinase inhibitors. *Bioorg. Med. Chem.* **2015**, *23*, 348-364.

35. Smith, C. R.; Dougan, D. R.; Komandla, M.; Kanouni, T.; Knight, B.; Lawson, J. D.; Sabat, M.; Taylor, E. R.; Vu, P.; Wyrick, C. Fragment-based discovery of a small molecule inhibitor of Bruton's tyrosine kinase. *J. Med. Chem.* **2015**, *58*, 5437-5444.

36. Young, W. B.; Barbosa, J.; Blomgren, P.; Bremer, M. C.; Crawford, J. J.; Dambach, D.; Gallion, S.; Hymowitz, S. G.; Kropf, J. E.; Lee, S. H.; Liu, L.; Lubach, J. W.; Macaluso, J.; Maciejewski, P.; Maurer, B.; Mitchell, S. A.; Ortwine, D. F.; Di Paolo, J.; Reif, K.; Scheerens, H.; Schmitt, A.; Sowell, C. G.; Wang, X.; Wong, H.; Xiong, J.; Xu, J.; Zhao, Z.; Currie, K. S. Potent and selective Bruton's tyrosine kinase inhibitors: Discovery of GDC-0834. *Bioorg. Med. Chem. Lett.* **2015**, *25*, 1333-1337.

37. Liu, J.; Guiadeen, D.; Krikorian, A.; Gao, X.; Wang, J.; Boga, S. B.; Alhassan, A. B.; Yu, Y.; Vaccaro, H.; Liu, S.; Yang, C.; Wu, H.; Cooper, A.; de Man, J.; Kaptein, A.; Maloney, K.; Hornak, V.; Gao, Y. D.; Fischmann, T. O.; Raaijmakers, H.; Vu-Pham, D.; Presland, J.; Mansueto, M.; Xu, Z.; Leccese, E.; Zhang-Hoover, J.; Knemeyer, I.; Garlisi, C. G.; Bays, N.; Stivers, P.; Brandish, P. E.; Hicks, A.; Kim, R.; Kozlowski, J. A. Discovery of 8-amino-imidazo[1,5-*a*]pyrazines as reversible BTK inhibitors for the treatment of rheumatoid arthritis. *ACS Med. Chem. Lett.* **2016**, *7*, 198-203.

38. De Lucca, G. V.; Shi, Q.; Liu, Q.; Batt, D. G.; Beaudoin Bertrand, M.; Rampulla, R.; Mathur, A.; Discenza, L.; D Arienzo, C.; Dai, J.; Obermeier, M.; Vickery, R.; Zhang, Y.; Yang, Z.; Marathe, P.; Tebben, A. J.; Muckelbauer, J. K.; Chang, C. J.; Zhang, H.; Gillooly, K.; Taylor, T.; Pattoli, M. A.; Skala, S.; Kukral, D. W.; McIntyre, K. W.; Salter-Cid, L.; Fura, A.; Burke, J. R.; Barrish, J. C.; Carter, P. H.; Tino, J. A. Small molecule reversible inhibitors of Bruton's tyrosine kinase (BTK): Structure–activity relationships leading to the identification of 7-(2-Hydroxypropan-2-yl)-4-[2-methyl-3-(4-oxo-3,4-

dihydroquinazolin-3-yl)phenyl]-9*H*-carbazole-1-carboxamide (BMS-935177). *J. Med. Chem.* **2016**, *59*, 7915-7935.

39. Katewa, A.; Wang, Y.; Hackney, J. A.; Huang, T.; Suto, E.; Ramamoorthi, N.; Austin, C. D.; Bremer, M.; Chen, J. Z.; Crawford, J. J.; Currie, K. S.; Blomgren, P.; DeVoss, J.; DiPaolo, J. A.; Hau, J.; Johnson, A.; Lesch, J.; DeForge, L. E.; Lin, Z.; Liimatta, M.; Lubach, J. W.; McVay, S.; Modrusan, Z.; Nguyen, A.; Poon, C.; Wang, J.; Liu, L.; Lee, W. P.; Wong, H.; Young, W. B.; Townsend, M. J.; Reif, K. Btk-specific inhibition blocks pathogenic plasma cell signatures and myeloid cell-associated damage in IFNα-driven lupus nephritis. *JCI Insight* **2017**, *2*, e90111.

40. Kawahata, W.; Asami, T.; Irie, T.; Sawa, M. Design and synthesis of novel pyrimidine analogs as highly selective, non-covalent BTK inhibitors. *Bioorg. Med. Chem. Lett.* **2018**, *28*, 145-151.

41. Crawford, J. J.; Johnson, A. R.; Misner, D. L.; Belmont, L. D.; Castanedo, G.; Choy, R.; Coraggio, M.; Dong, L.; Eigenbrot, C.; Erickson, R.; Ghilardi, N.; Hau, J.; Katewa, A.; Kohli, P. B.; Lee, W.; Lubach, J. W.; McKenzie, B. S.; Ortwine, D. F.;

Schutt, L.; Tay, S.; Wei, B.; Reif, K.; Liu, L.; Wong, H.; Young, W. B. Discovery of GDC-0853: A potent, selective, and noncovalent Bruton's tyrosine kinase inhibitor in early clinical development. *J. Med. Chem.* **2018**, *61*, 2225-2245.

42. Liu, L.; Halladay, J. S.; Shin, Y.; Wong, S.; Coraggio, M.; La, H.; Baumgardner, M.; Le, H.; Gopaul, S.; Boggs, J.; Kuebler, P.; Davis, J. C.; Liao, X. C.; Lubach, J. W.; Deese, A.; Sowell, C. G.; Currie, K. S.; Young, W. B.; Khojasteh, S. C.; Hop, C. E. C. A.; Wong, H. Significant species difference in amide hydrolysis of GDC-0834, a novel potent and selective Bruton's tyrosine kinase inhibitor. *Drug Metab. Dispos.* **2011**, *39*, 1840-1849.

43. Wu, H.; Huang, Q.; Qi, Z.; Chen, Y.; Wang, A.; Chen, C.; Liang, Q.; Wang, J.; Chen, W.; Dong, J.; Yu, K.; Hu, C.; Wang, W.; Liu, X.; Deng, Y.; Wang, L.; Wang, B.; Li, X.; Gray, N. S.; Liu, J.; Wei, W.; Liu, Q. Irreversible inhibition of BTK kinase by a novel highly selective inhibitor CHMFL-BTK-11 suppresses inflammatory response in rheumatoid arthritis model. *Sci. Rep.* **2017**, *7*, 466.

44. Bradshaw, J. M.; McFarland, J. M.; Paavilainen, V. O.; Bisconte, A.; Tam, D.; Phan, V. T.; Romanov, S.; Finkle, D.; Shu, J.; Patel, V.; Ton, T.; Li, X.; Loughhead, D. G.; Nunn, P. A.; Karr, D. E.; Gerritsen, M. E.; Funk, J. O.; Owens, T. D.; Verner, E.; Brameld, K. A.; Hill, R. J.; Goldstein, D. M.; Taunton, J. Prolonged and tunable residence time using reversible covalent kinase inhibitors. *Nat. Chem. Biol.* **2015**, *11*, 525-531.

45. Reiff, S. D.; Muhowski, E. M.; Guinn, D.; Lehman, A.; Fabian, C. A.; Cheney, C.; Mantel, R.; Smith, L.; Johnson, A. J.; Young, W. B.; Johnson, A. R.; Liu, L.; Byrd, J. C.; Woyach, J. A. Noncovalent inhibition of C481S Bruton tyrosine kinase by GDC-0853: a new treatment strategy for ibrutinib-resistant CLL. *Blood* **2018**, *132*, 1039-1049.

46. Watterson, S. H.; De Lucca, G. V.; Shi, Q.; Langevine, C. M.; Liu, Q.; Batt, D. G.; Beaudoin Bertrand, M.; Gong, H.; Dai, J.; Yip, S.; Li, P.; Sun, D.; Wu, D. R.; Wang, C.; Zhang, Y.; Traeger, S. C.; Pattoli, M. A.; Skala, S.; Cheng, L.; Obermeier, M. T.; Vickery, R.; Discenza, L. N.; D'Arienzo, C. J.; Zhang, Y.; Heimrich, E.; Gillooly, K. M.; Taylor, T. L.; Pulicicchio, C.; McIntyre, K. W.; Galella, M. A.; Tebben, A. J.;

Muckelbauer, J. K.; Chang, C.; Rampulla, R.; Mathur, A.; Salter-Cid, L.; Barrish, J. C.; Carter, P. H.; Fura, A.; Burke, J. R.; Tino, J. A. Discovery of 6-fluoro-5-(R)-(3-(S)-(8-fluoro-1-methyl-2,4-dioxo-1,2-dihydroquinazolin-3(4H)-yl)-2-methylphenyl)-2-(S)-(2-hydroxypropan-2-yl)-2,3,4,9-tetrahydro-1H-carbazole-8- carboxamide (BMS-986142): A reversible inhibitor of Bruton's tyrosine kinase (BTK) conformationally constrained by two locked atropisomers. *J. Med. Chem.* **2016**, *59*, 9173-9200.

47. Neffendorf, J. E.; Gout, I.; Hildebrand, G. D. Ibrutinib in relapsed chronic lymphocytic leukemia. *N. Engl. J. Med.* **2013**, *369*, 1258-1259.

48. Byrd, J. C.; Brown, J. R.; O Brien, S.; Barrientos, J. C.; Kay, N. E.; Reddy, N. M.; Coutre, S.; Tam, C. S.; Mulligan, S. P.; Jaeger, U. Ibrutinib versus ofatumumab in previously treated chronic lymphoid leukemia. *N. Engl. J. Med.* **2014**, *371*, 213-223.

49. O'Brien, S.; Furman, R. R.; Coutre, S. E.; Sharman, J. P.; Burger, J. A.; Blum, K. A.; Grant, B.; Richards, D. A.; Coleman, M.; Wierda, W. G. Ibrutinib as initial therapy for elderly patients with chronic lymphocytic leukaemia or small lymphocytic lymphoma: an open-label, multicentre, phase 1b/2 trial. *Lancet Oncol.* **2014**, *15*, 48-58.

50. Lu, D.; Chambers, P.; Wipf, P.; Xie, X.-Q.; Englert, D.; Weber, S. Lipophilicity screening of novel drug-like compounds and comparison to cLog P. *J. Chromatogr. A* **2012**, *1258*, 161-167.

51. Bohm, H. J.; Banner, D.; Bendels, S.; Kansy, M.; Kuhn, B.; Muller, K.; Obst-Sander, U.; Stahl, M. Fluorine in medicinal chemistry. *ChemBioChem* **2004**, *5*, 637−643.

52. Boucheron, N.; Ellmeier, W., The Role of Tec family kinases in the regulation of T-helper-cell differentiation. *Int. Rev. Immunol.* **2012**, *31*, 133-154.

Table of Contents graphic

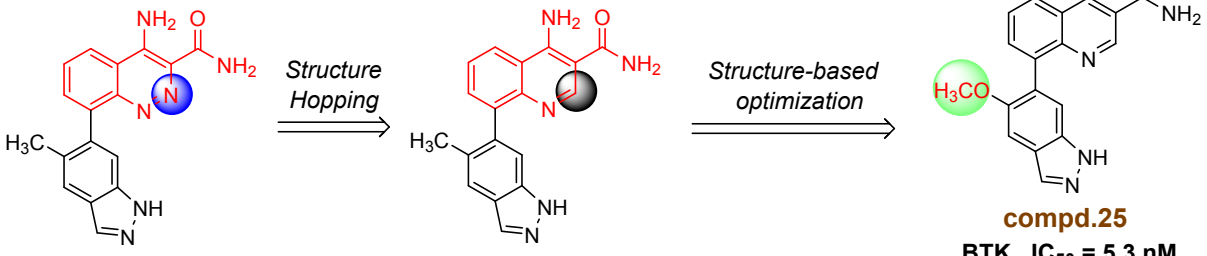

compd.6
cinnoline scaffold
Aq. Sol. < 0.05 μg/mL

compd.7
quinoline scaffold
Aq. Sol. = 10.5 μg/mL
Solubility improved > 200 fold

compd.25
BTK IC_{50} = 5.3 nM
BTK *C481S* IC_{50} = 39 nM
Aq. Sol. = 7.3 μg/mL
***In vivo* anti-RA**
Plasma recovery % (human,rat, monkey,mouse,dog) > 88%